Carolina Pinto Inverno da Piedade

Licenciatura em Ciências da Engenharia Biomédica

Past/present and future worries: an fMRI study

Dissertação para obtenção do Grau de Mestre em
Engenharia Biomédica

Orientador: Gina Caetano, Investigadora Auxiliar, IBILI/ICNAS – UC

Co-orientadores: Miguel Castelo-Branco, Director, IBILI/ICNAS – UC
Pedro Vieira, Professor Auxiliar, FCT-UNL

Júri:

Presidente: Professora Doutora Carla Maria Quintão Pereira

Arguente: Professor Doutor Mário António Basto Forjaz Secca

Vogal: Professora Doutora Gina Maria Costa Caetano

FACULDADE DE CIÊNCIAS E TECNOLOGIA
UNIVERSIDADE NOVA DE LISBOA

Dezembro, 2014

Past/present and future worries: na fMRI study

To my lovely parents

Acknowledgements

This work was supported by Fundação para a Ciência e Tecnologia (PTDC/SAU-BEB/100147/2008, Pest-C/SAU/UI3282/2013), Portugal.

I would like to thank Professor Gina Caetano for her expert advise, dedication and encouragement throughout this project. It was a great pleasure to learn so much with your precious help.

I am also grateful to Professor Miguel Castelo-Branco, Director of ICNAS/IBLI, who created the experimental protocol and made this work possible by accepting me.

I would also want to thank Professor Mário Secca for his dedication to Biomedical Engineering and for the captivating way he transmits his knowledge about Magnetic Resonance Imaging.

I am thankful to Daniel Ruivo, who has developed the evaluation protocol and experimental design, for all the support, availability and patience throughout the endless hours spent in data transference. I also want to thank Catarina Duarte for the MatLab implementation, as well as João Marques and Carlos Ferreira for technical support in MR acquisitions.

I thank Bernardo for his friendship and company throughout our adventure in Coimbra where I met so many good and unforgettable friends.

I am grateful for the amazing friends I met in FCT-UNL during this five year journey. Particularly, I thank Carolina for all the fun and honest moments and Nuno for the companionship, support and for always managing to make me laugh.

I would like to thank my sister Leonor, for her unconditional friendship and for inspiring me every day with her hard work.

Last but not least, I am grateful to my parents, Fernando and Luísa for their absolute love and support. Thank you for being the perfect example and for encouraging me to be better and to follow my dreams.

Resumo

Na última década, o conhecimento sobre a estrutura e funções cerebrais foi alvo de um notável avanço, principalmente devido às numerosas técnicas de neuro-imagem desenvolvidas. De entre os estudos relacionados com a neurociência, são cada vez mais comuns os estudos de neuropsiquiatria com recurso e imagem médica funcional.

O presente estudo tem como principal foco a identificação das áreas cerebrais recrutadas enquanto sujeitos controlo leem frases com as suas preocupações pessoais acerca do passado/presente e do futuro. O principal objetivo é caracterizar, de forma rigorosa e em condições controlo, estas áreas cerebrais por forma a explorar as implicações de relembrar acontecimentos passados/presentes ou pensar em preocupações relacionadas com o futuro. Com isto em mente, imagens de ressonância magnética funcional foram recolhidas de dez indivíduos saudáveis. Os dados adquiridos foram processados e tratados estatisticamente com recurso ao Modelo Linear Geral, ao Modelo de Efeitos Fixos e ao Modelo de Efeitos Aleatórios. Posteriormente, uma análise multi-voxel com uma técnica de "Seachlight Mapping" foi executada com o intuito de encontrar padrões de ativação cerebrais que permitissem a diferenciação entre as condições estudadas.

Os resultados obtidos indicaram prevalência de ativação cerebral durante a leitura de frases referentes a preocupações passadas/presentes em comparação com preocupações futuras e frases de conteúdo neutro. As principais áreas identificadas estão situadas no córtex frontal, bem como nas áreas parietais, occipitais e temporais posteriores. A preocupação, por si só, mostrou ativação do córtex parietal posterior e medial, lóbulo occipital esquerdo posterior, e do lóbulo temporal esquerdo. A análise multi-voxel permitiu identificar padrões de distinção entre condições situados principalmente nos lóbulos parietal, límbico e frontal.

Palavras-chave: fMRI, preocupação, pensamentos sobre o futuro, lembranças do passado

Abstract

For the past decade, numerous imaging techniques gave rise to remarkable progresses in the understanding of brain's structure and function. Amongst the wide variety of studies onto the field of neuroscience, neuropsychiatric researches with resource to neuroimaging have attracted increasing attention.

The present study will focus on the identification of brain areas recruited while normative subjects read sentences related to past/present or future worries. Our main aim was to accurately characterize these brain areas while providing them with a time-stamp that would hopefully help us understand the implications of past/present memories and future envisioning in worrying episodes. With that purpose, functional magnetic resonance imaging data was collected from ten healthy individuals. The obtained data was processed and statistically treated using the General Linear Model and both Fixed and Random Effects Analysis for group-level results. Thereafter, a Multi-Voxel Pattern Analysis with Searchlight Mapping was performed in order to find patterns of activation that allow differentiation between conditions.

The obtained results indicate higher brain activation while reading sentences related to past/present worries when compared to future worry or neutral sentences. The main areas include frontal cortex, posterior parietal, occipital and temporal areas. Worrying, per se, was characterized by activation of the medial posterior parietal cortex, left posterior occipital lobe and left central temporal lobe. With the searchlight mapping approach we were able to further identify patterns of distinction between conditions, which were located in the parietal, limbic and frontal lobes.

Keywords: worry, episodic future thoughts, past events recollection, fMRI

List of Contents

Abbreviations

3D – Three-Dimentions

4D – Four-Dimentions

AC – Anterior Commissure

AR – First Order Autoregressive

BA – Brodmann Area

EPI – Echo-planar Imaging

FA – Fine-Tuning Alignment

FDR – False Discovery Rate

FFX – Fixed Effects Analysis

fMRI – Functional Magnetic Resonance Imaging

FWER – Family-wise Errors

GAD – General Anxiety Disorder

GLM – General Linear Model

HRF – Hemodynamic Response Function

IA – Initial Alignment

IIHC – Intensity Inhomogeneity Correction

MRI – Magnetic Resonance Imaging

MVPA – Multi-Voxel Pattern Analysis

N – Neutral

OCD – Obsessive Compulsive Disorder

PC – Posterior Commissure

PCC – Posterior Cingulate Cortex

PET – Positron Emission Tomography

PM – Percent Accuracy

rCBF – Regional Cerebral Blood Flow

RFX – Random Effects Analysis

ROI – Region-of-interest

SMA – Supplementary Motor areas

SVM – Support vector machine

T_2* - Real Transverse Relaxation Time

TE – Echo time

TR – Repetition time

V1 – Primary Visual Cortex

V2 – Secondary Visual Cortex (Area 2)

WR– Worrying related

List of Figures

List of Tables

1

State of the Art and Motivation

1.1) Neural Correlates of past/present events retrieval and future envisioning

The ability to mentally simulate an episode is common to every healthy human being. This remarkable capability allows us to remember and vividly represent, within our own imagination, personal events that occurred in the past. Moreover, it allows us to envision the outcomes of a possible future situation.

Mental imagery is thought to be granted mainly by a wide archive: our memory system. We recollect pieces of information that combined form coherent representations of different events. This recombination may be more or less flexible depending on whether we are attempting to envision something that may occur or simply trying to remember something that has already happened. Either way, since the archive is the same, various neuroscientists believe that past recollection and episodic future thought have the same neurologic basis and serve as complementary functions at one's ability to mentally travel over time (Szpunar et al. (2006), Botzung et al. (2008), Andrews-Hanna et al. (2014)).

Several studies have been performed in which subjects were asked to talk about or just imagine past, present or future events while undergoing neuroimaging exams such as Positron Emission Tomography (PET) (Okuda et al.

(2003)) and Functional Magnetic Resonance Imaging (fMRI) (Szpunar et al. (2006), Addis et al. (2007), Botzung et al. (2008), Viard et al (2010)). The great majority of these studies were, in fact, able to identify brain areas that seemed to be recruited equally while envisioning past and future events.

Mentally constructing an episode (independently of its associated time-stamp) appears to involve the activation of brain areas situated mainly in the medial posterior cortex and the medial temporal lobe (Okuda et al. (2003); Szpunar et al. (2006); Botzung et al. (2008); Addis et al. (2007); Andrews-Hanna et al. (2014)) and some parts of the left hippocampus (Addis et al. (2007)). More specifically, the right inferior parietal lobule (BA 39 and 40), left superior occipital gyrus/cuneus (BA 18) and right middle occipital gyrus (BA 19) (Addis et al. (2007)) showed similar patterns of activation during past recollection and future imagining. The medial surface of the temporal lobe forms a system of structures thought to be mainly concerned with memory, with special emphasis to declarative memory (conscious memory for facts and events). The hippocampus is an important part of this system and seems to have an important role in combining information from multiple sources (for instance, while recollection of specific events from the episodic memory system). The noted existence of highly similar patterns of brain activation involved in both future and past episodic construction corroborated the idea that the ability to mentally travel along the axis of one's own subjective time can only be possible through the act of combining and recombining basic mnemonic elements to generate a complex mental image. In that case, the temporal areas recruited would be responsible for the recollection and recombination of memory elements to form an event, while the visual processing areas (BA 18 and 19) would be involved in the construction of the event's mental representation (Addis et al. (2007)). As the parietal areas recruited were reported to be mostly concerned with attention, their function in memory may involve orienting attention to internal memory representation (Addis et al. (2007)).

Deep reflection and elaboration regarding the previously constructed mental episodes also proved to have similar neural correlates for both past retrieval and future thoughts. The brain regions recruited, however, revealed to be mainly located in the medial prefrontal cortex (Szpunar et al. (2006); Botzung

et al. (2008); Addis et al. (2007); Andrews-Hanna et al. (2014)). Past and future elaborations were shown to have the same level of activation in the autobiographic memory network, which is composed by frontopolar (BA 10) and inferior (BA 11) aspects of the left medial prefrontal cortex, left temporal pole (BA 38) and middle temporal gyrus (BA 20/21), left hippocampus, bilateral parahippocampal gyrus, bilateral posterior cingulate (BA 29, 30 and 31), left precuneus (BA 7), bilateral anterior parietal lobule (BA 39) and cerebellum (Addis et al. (2007)).

Once studies suggest preferential recruitment of the prefrontal cortex for self-referential mental activity, it is plausible to hypothesize that, in order to generate plausible images of the past or future one must reactivate images previously kept in the posterior cortex (Szpunar et al. (2006); Addis et al. (2007)) Furthermore, the involvement of both prefrontal and posterior subsystems in autobiographical tasks reinforces the hypothesis that episodic retrieval and mentalizing play an important role in recalling one's past and imagining one's future.

On the other hand, researchers were able to identify some areas more potentially involved in extracting future prospects than collecting past experiences during construction and elaboration of metal episodes. In the construction phase, the differentiation of past and future were maximal (when compared with the elaboration phase) with prevalence of the future envisioning. The brain regions recruited during construction were right hippocampus (Okuda et al. (2003); Addis et al. (2007)), right hemispheric BA 10 and left BA 11 from the frontopolar cortex (Okuda et al. (2003); Addis et al. (2007)), and some motor areas such as lateral premotor cortex, medial posterior parietal cortex and posterior cerebellum (Szpunar et al. (2006)). The posterior right middle temporal gyrus and left inferior parietal lobule were greatly activated in the elaboration of future thought (Addis et al. (2007)).

An fMRI study by Botzung et al. (2008) corroborated the existence of highly similar patterns of activation involved in both episodic future thought and past event recollection. However, this is one of the few studies to report greater activity of hippocampal and anterior medial prefrontal areas during elaboration of past episodic thought. Botzung et al. (2008) suggested that past

events recollection might be associated with greater self-involvement when compared with episodic future. From this perspective, the act of reflecting about an experienced personal event involves more details, thoughts and feeling associated than just imagining something that has not even occurred yet.

Considering the reviewed literature, we might suggest that there are two major lines of results across studies: one defending that envisioning the future encompasses more intense recruitment of certain brain regions (Okuda et al. (2003), Addis et al. (2007), Szpunar et al. (2006)); and another which states that recollecting and reflecting on past episodes require greater amount of activation in certain cerebral (Botzung et al. (2008)). Several factors may underlie this fundamental controversy such as, for instance, the chosen experimental paradigm or the imaging method itself.

We resort to recollection of past events and envision of future episodes on a regular basis, countless times a day, intentionally or not. In fact, the human brain is thought to have a certain amount of activity at any given time, even when an individual is at a resting state. When the brain is at a wakeful rest, studies have shown that its default mode network is always active, performing task-independent introspection. Moreover, recent researches about these self-referential thoughts that characterize the resting brain have been able to link them with associative processing involving recollection of past/present memories and envisioning the future.

This nearly permanent mental travelling is often engaged when we worry about some event from our everyday life. For instance, when we don't feel comfortable about something that has occurred, or when we feel anxious about a future situation.

Since worrying involves mainly self-referential negative thoughts and is evermore related with past or upcoming events, it is plausible to foresee that different time-related types of worrying will incite the activity of different brain regions.

1.2) Neural Correlates of worry and rumination in healthy controls

Worrying is a relatively common feeling, experienced in a great variety of situations, pathologic or not. It characterizes anxious apprehension (the mildest type of anxiety that seems to underlie the worrying states) and encompasses repetitive thoughts which may be related to personal and emotional threats to self, competence at work or general world problems (Engels et al. (2007)). Worrisome thoughts appear to constitute an attempt to prevent or minimize negative emotions related to unpleasant images (Hofmann et al. (2005)). Furthermore, the worrying state is associated with conscious exaggerated threat appraisal and is thought to encompass negative estimates of distant, uncertain and unpredictable dangers that may accrue from either self-relevant aspects or external threats (Kalisch et al. (2014)). When a self-related thought is generated, the anxiety and negative emotionality experienced escalate rapidly and tend to be maintained for long periods of time (Kalisch et al. (2014)). Berenbaum et al. (2010) created a detailed two-step initiation-termination model to characterize the process of worrying. According to him, in an initial phase, the worrying state is generated when an individual perceives a threat and becomes aware of its potential undesirable outcome. Intuitively, the greater the threat, the more likely is worrying to be initiated. The second phase of this model, the termination phase, involves the acceptance of the prospect of the threat. Accepting the inevitability of a danger or risk seems to provide a certain sense of closure to the worrying individual and terminates his anxiety state.

According to important studies onto this subject, anxious apprehension involves mostly verbal and cognitive components and is characterized by larger frontal asymmetry in favor of the left hemisphere (Hofmann et al. (2005); Engels et al. (2007)).

Paulesu et al. (2010) were able to further substantiate the existence of specific brain regions for worry-oriented thoughts using BOLD fMRI. Their study pinpointed some brain areas recruited when normal controls were asked to exclusively generate thought in response to worry-inducing sentences, such as: the superior frontal medial gyrus (BA 10), the inferior frontal medial orbital

gyrus (BA 10) and the anterior cingulate cortex (BA 25). Overall, for both auditory and visual stimuli that induced worry, their research allowed the identification of several worry-related brain areas, most of which medial regions of the frontal lobe. These findings were particularly interesting because the spotted areas are thought to be related to reflection of one's own mental state and on mental states of others.

Several studies addressed more specifically which brain regions were activated and deactivated during worrying. Overall, during worrisome thoughts, the rostral dorsal anterior cingulate and rostral dorsomedial prefrontal cortex proved to be hyper-activated whereas the limbic system and some occipito-temporal areas showed less activation (Hoehn-Saric et al. (2005); Paulesu et al. (2009); Kalisch et al. (2014)). In their review, Kalisch et al. (2014) narrowed the search for the brain regions that mediate worrying, and hypothesized that the rostral dorsal anterior cingulate and rostral dorsomedial prefrontal cortex should be hyper-activated during this sort of emotional state. In other research work, Hoehn-Saric et al. (2005) measured regional cerebral blood flow (rCBF) with PET in non-anxious individuals who expressed everyday life worries. Their results showed that, compared to neutral thinking, worrisome thoughts led to significant increase in rCBF in the right thalamus and bilateral (with left predominance) orbito-frontal gyrus. Moreover, decreases in rCBF during worrying were observed in the right amygdala, hippocampus and insula, left and right superior, middle and inferior temporal gyri, the left anterior temporal tip, the left supramarginal and angular gyri, the left and right occipito-temporal gyrus and the inferior occipital gyrus. The increase versus decrease of rCBF between prefrontal regions and the limbic system, respectively, led the authors to suggest that there is, in fact, a cause-effect relation affecting the activation of certain areas and inhibition of others during worrying thoughts. This negative correlation may lead to the conclusion that greater integrative and cognitive efforts to find a solution for a worry-inducing situation are responsible for the inhibition of the limbic system in healthy subjects.

Some individuals have an unusual tendency to worry, which means they may find it difficult to perform the cognitive tasks that allow them to terminate the process of worrying. In some cases, this tendency is so overwhelming that ultimately gives rise to psychiatric disorders such as Depression, Obsessive Compulsion Disorder (OCD) and, specially, General Anxiety Disorder (GAD) (Davey and Wells (2006)).

Studying and understanding this type of emotional states is highly important, not only because they are common aspects of almost all individuals' lives but because of the important role they play in many forms of psychopathology.

1.3) Clinical Applications

Anxiety disorders have been studied using functional imaging techniques. As they are highly common psychiatric disorders (Garner et al. (2009), Moreno-Peral et al. (2014)), understanding and characterizing them at neuronal levels may contribute to more adequate medical treatments and therapies. The central symptom shown by patients with psychopathologies such as General Anxiety Disorder is worry (Paulesu et al. (2010)). Some studies, that compare subjects with generalized anxiety disorder (GAD) and normal controls, have shown that in both groups the same brain region usually undergoes activation during worrying thoughts (Paulesu et al. (2010), Andreescu et al. (2011)). In GAD patients this activation tends to extend itself over time, even during relaxation phases, which suggests that GAD subjects may have an inability to recognize the moment in which it would be useful to stop worrying (Paulesu et al. (2010)).

A more specific study, with elderly subjects, was able to identify additional brain regions that were activated during worrying, including the right insula, bilateral amygdala and associative temporo-occipital areas (Andreescu et al. (2011)). Measures of regional cerebral blood flow using Pulsed Arterial

Spin Labeling perfusion MRI spotted a lack of recruitment of certain prefrontal cortical areas responsible for worry suppression in elderly GAD subjects (Andreescu et al. (2011)). This evidenced that pathologic worry may be associated with a greater difficulty in successfully stopping brain's processes involved in worrying.

1.4) Motivation

The present study will focus on the identification of brain areas recruited while normative subjects read sentences related to past/present or future worries. Our main aim is to accurately characterize these brain areas in normal conditions while providing them with a time-stamp that would hopefully help us understand the implications of past/present memories and future envisioning in worrying episodes. With that purpose blood-oxygen-level dependent (BOLD) signals will be collected within a healthy population sample using functional magnetic resonance imaging (fMRI).

1.5) Functional Magnetic Resonance Imaging: An Overview

The information on the present subchapter is based upon Scott A. Huettel and colleges' textbook: "Functional Magnetic Resonance Imaging"; chapters 1, 6, 7 and 8.

Functional magnetic resonance imaging constitutes an indirect method to evaluate brain activation. This technique takes into consideration the correlation between local blood flow variation and neuronal activation to study brain's functioning during execution of a certain task. The functional data obtained is usually corregistered on high-resolution anatomical images in order to allow proper localization of the activated brain areas.

➢ Basic Principles

Neuronal activity requires oxygen which is transported by blood's hemoglobin throughout the circulatory system. Therefore, in brain's activated areas, the oxygen consumption rate is higher than normal which triggers body's compensatory mechanisms to increase blood flow and, consequently, oxygen supply in the area. Since these compensatory mechanisms often exceed the requirements, the increasing blood flow leads to an abnormal augmentation in oxygenated hemoglobin's (Hb) concentration in the activation area. Additionally, the concentration of deoxygenated hemoglobin (dHb) in the same area will be unusually low. Consequently, Hb/dHb ratio will increase which seems to characterize neuronal activity.

Deoxygenated hemoglobin has paramagnetic properties responsible for the generation of microscopic magnetic fields within the MR scanner, causing heterogeneities in the main magnetic field. However, the decreasing proportion of dHb during activation counteracts those heterogeneities, increasing tissues' characteristic real transverse relaxation time, T_2*. Using MRI T_2* contrast techniques, it is possible to identify significant increases in signal's intensity in brain activation regions, which become localizable.

➢ Blood–Oxygenated–Level Dependent Technique (BOLD)

Several fMRI studies, including the present one, use a blood-oxygenation-level dependent technique (BOLD). This approach takes into consideration the increasing signal in brain regions with high Hb/dHb ratio to find presumable cerebral activations with resort to T_2* contrast techniques. We assume that the BOLD signal amplitude is proportional to neuronal activation and generally represent it in function of time by a hemodynamic response function (HDR).

- **Hemodynamic Response Function (HRF)**

Generally, for a short stimulus, HRF may be represented by Figure1.1.

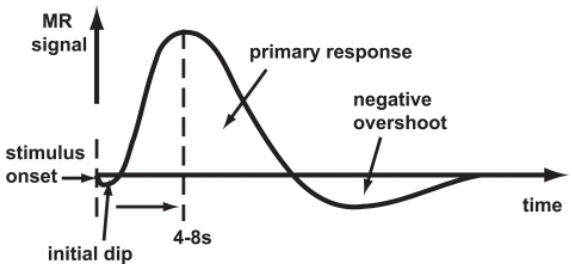

Figure 1.1: An example of an Hemodynamic Response Fucntion regarding a short stimulus (collected from Kornak et al. (2011))

In Figure 1.1, the decrease in signal verified immediately after the stimulus ("initial dip") is due to the sudden increase in oxygen consumption when neuronal activity is initiated. Shortly after, once the compensatory mechanisms take action, BOLD signal increases, thus forming the function's peak.
With the end of the stimulus, neuronal activity ceases and other compensatory mechanisms are stimulated this time in order to guarantee the diminution of local blood flow. As a consequence, BOLD signal decreases. The "negative overshoot" present in Figure 1.1 evidences the exaggerated vessel constriction (an effect of the compensatory mechanisms) which leads to an abnormally lower Hb/dHb ratio. Body's compensatory mechanisms take some seconds to reestablish normal blood flow (BOLD signal's baseline).

In conclusion, it should be noted beforehand that BOLD fMRI does not recognize neuronal activity per se, but the metabolic demand of active neurons.

1.6) Methods for Statistical Analysis of fMRI data

Neuroimaging studies using fMRI give rise to massive amounts of data with its unavoidable noise and artifacts derived from countless sources. Hence, statistics play a crucial role in understading the nature of the data and accessing

its relevance, providing neuroscientists with important interpretational information. In this chapter we will illustrate interesting and important issues in which statistics are critical for fMRI data manipulation.

➢ Single Subject Analysis

In order to truly understand the nature of BOLD signal, and, specially, to localize brain activity, it is essential to establish three background assumptions. First of all, the signal provides a measure of the amplitude of neuronal activity under a certain condition. This implies that fMRI signal will be scaled by a factor if the input (the neuronal activity) is scaled by the same factor. Secondly, fMRI signal is cumulative, i.e. the response to two different stimuli applied together equals the sum of the individual responses to each stimulus individually. And, finally, when a stimulus is shifted by a time t, the response is also shifted by t, hence, fMRI signal is time-invariant. All previously mentioned assumptions form the baseline from which it is possible to start handling fMRI data and, hopefully, draw meaningful conclusions. Namely, distinguish between highly and slightly activated brain areas, and discriminate data from different conditions.

In the present work, the method used to single subject's fMRI statistical analysis is the General Linear Model (GLM).

The General Linear Model

The general linear model is the univariate statistical method (introduced in the neuroscience community by Friston et al. (1994)) that underlies most fMRI data analysis. It is a multiple regression technique which evaluates the relative contributions of all processes that may be involved in the generation of the observed data, y_i. Since GLM assumes that both stimulus function and Hemodynamic Response Function are known a priori, the referred processes, also known as predictors, may be written in a reference function, X_{ij}, obtained by convoluting the condition box-car time course predicted by the protocol with a standard hemodynamic response function. On the other hand, as the

noise is present within each voxel, an error or residual function, e_i, must also be built. Since each predictor has different quantitative contributions to the observed data, they are associated with individual weighting factors, β_j.

The ultimate purpose of the GLM analysis is to find the predictor's weighting factors that best accounts for the original data by minimizing the error or residual terms. The following equations represent the linear correlations performed in this regression technique:

$$
\begin{aligned}
y_1 &= \beta_0 + \beta_1 X_{11} + \beta_2 X_{12} + \cdots \beta_p X_{1p} + e_1 \\
y_2 &= \beta_0 + \beta_1 X_{21} + \beta_2 X_{22} + \cdots \beta_p X_{2p} + e_2 \\
y_3 &= \beta_0 + \beta_1 X_{31} + \beta_2 X_{32} + \cdots \beta_p X_{3p} + e_3 \\
&\cdots \\
y_n &= \beta_0 + \beta_1 X_{n1} + \beta_2 X_{n2} + \cdots \beta_p X_{np} + e_n
\end{aligned}
$$

Equation 1.1

The weighting of each physiologic parameter as well as the error terms are calculated for each voxel independently. The first β value, β_0, typically represents the signal level of the baseline condition.

The physiologic processes' hypothesized changes over time (as a result of the different stimuli underwent by the subjects during the fMRI scanning), related to the expected hemodynamic response in time, may also be represented in a design matrix, G, with n rows (number of hemodynamic peaks during the entire scanning) and M columns (number of physiologic processes). On the other hand, as the noise is present within each voxel, the error matrix, ε, will also have n rows but V columns (the number of voxels in the imaging volume). The time evolution of the fMRI data is also arranged in a two-dimensional matrix with n rows and V columns and is known as the data matrix, Y. Finally, the weighting factors form the parameter matrix, β, with V rows and M columns (the number of physiological processes is equal to the name of weighting factors). The multiple regression equations performed in the GLM may be represented as one simple equation containing all four matrices previously mentioned (Equation 1.2).

$$Y = G \times \beta + \varepsilon$$

Equation 1.2

GLM's residual time course typically exhibits serial correlations, i.e. high values followed more likely by high values than low values and vice versa. Serial correlations violate the assumption of uncorrelated errors, and probably occur due to the rapid succession of data point's measurement. However, since GLM expects the original voxel time course to present this type of biased information, its correction is done effectively during this statistical operation. Therefore, the estimated beta values are unbiased. Nevertheless, the standard errors of beta values are biased resulting in an abnormal increase in t-values obtained. In order to avoid this sort of errors, it is possible to correct serial correlations using a pre-whitening approach in which autocorrelation is estimated by assuming the errors follow a first-order autoregressive, or AR(1), process. In this approach, GLM is calculated normally, subsequently estimating the amount of serial correlations, *r*, using a pair of successive residual values (the time course of a certain residual is correlated with itself shifted by one time point). Measured voxel's time course (y_t) is then re-adjusted and a transformed time course (y_t^n) is calculated by removal of the estimated *r* values (as can be seen in Equation 1.3)

$$y_t^n = y_{t+1} - r.y_t$$

Equation 1.3

The design matrix is re-adjusted as well by applying the same calculation to each predictor's time course. Finally, correct standard errors for beta estimates and correct significance levels (*t*-values) are obtained by re-computation of the GLM using the corrected voxel time courses and the adjusted design matrix.

The GLM approach relies on theoretical HRF to generate a set of regressors and build a design matrix. Thereafter, it determinates how strongly each of the regressors matches changes in the measured BOLD signal. This signal

does not provide information about absolute levels of brain activation. Instead it represents the changes in activation over time. Therefore, it is necessary to compare activation between two or more experimental conditions by statistical evaluating if the experimental alterations evoke significant changes in the overall cerebral activation. This evaluation is called contrast, and it may be in relation to baseline activity or between experimental tasks.

Although simple, GLM represents a powerful and rigid approach towards modulating data. However, due to the massive amount of data, examining the appropriateness of the model is challenging and standard methods of model diagnostics are not feasible.

➢ Group-Level Analysis

So far we have focused on the statistical methods to identify areas of activation within a single subject's brain. However, the majority of fMRI research (the present study included) fundamentally aim to identify the recruited brain areas in a certain experimental condition and generalize their activation within a sampled population (with specific features that characterizes the group). Nonetheless, combining data from multiple subjects presents more than a few challenges, which is why it is important to choose the more adequate statistical approach for intersubject analysis.

The main two statistical methods for multisubject fMRI data analysis are: Fixed Effects Analysis (FFX) and Random Effects Analysis (RFX).

Fixed Effects Analysis

FFX is the more intuitive method since it assumes that, apart from random noise, the experimental effects are constant across subjects. From this point of view, it is possible to combine all data points as well as the corresponding design matrices (previously obtained with GLM) from all subjects in a single statistical significance test. As a result, we obtain a brain map in which regions' average activation across subjects is evidenced.

This method offers great sensitivity and statistical power, thus presenting a popular way to analyse intersubject fMRI data. However, when exclusively used, it fails to provide information applicable to the general population, implying that the obtained results are strictly valid only for the investigated group. Intuitively, that happens because when choosing to resort to an average approach, one may be neglecting some subject's pieces of information substantially different from the majority of the data, thus resulting in misleading conclusions.

Random Effects Analysis

In order to be able to generalize the data to the population from which the sample of subjects have been drawn, a random effects group analysis has to be performed. This statistical approach explicitly models the inter-subject variability by considering each subject merely as one of the many possible participants who could have taken part in the experiment.

Although FFX is a highly sensitive method due to its substantially greater amount of considered degrees of freedom, RFX is a much more appropriate model to achieve relevant and credible results.

The Multiple Comparisons Problem

During the massive amount of statistical tests performed during fMRI data analysis, there are thousands of voxels that end up by showing statistical significance by chance (false-positives). The increase in the number of false-positives, also known as family-wise errors, results from increasing number of statistical tests and is known as Multiple Comparisons Problem.

It is then crucial to control the family-wise errors rate (FWER) by applying multiple comparisons correction methods that mainly calculate the appropriate statistical significance threshold (alpha value). A detailed characterization of the most commonly used multiple comparison correction methods, in neuroimaging, may be consulted in Appendix 1.

➢ Multi-Voxel Pattern analysis

Unlike GLM, in which a condition effect is analyzed voxel by voxel, the Multi-Voxel Pattern analysis (MVPA) allows the collective analysis of individual voxels within a region. MVPA methods offer higher sensibility in detecting and comparing different activation patterns between conditions. These tools are often referred to as classifiers or "learning machines" since they are capable of analyzing a set of fMRI activity patterns that may describe specific mental states and classify them within a finite group of possibilities. Obviously, the classification process in not random and must follow certain rules which are built in MVPA's "learning phase". At this point, fMRI data is divided in two sets. One "training" set used to estimate conditions that provide the match between brain activation patterns (input) and the corresponding class labels (target), thus providing a mapping function of the brain (a vector with N elements, in which each element specifies the presence of a certain feature measured within each one of the N voxels included in the analysis); and another "test" set which will be classified (one previously defined label will be assigned to each new fMRI activation pattern) using the created mapping function. At the end of the learning phase, the classifier should be able to correctly classify new submitted data, as well as the learned and tested activity patterns.

Searchlight Mapping

Since each activation pattern used during the learning phase is represented as a feature vector with N elements, for whole-brain mapping, a great number of activation patterns with high N must be used as learning set, thus resulting in low generalization accuracies because of the large amount of "noise" voxels (those voxels whose activation is not relevant). In order to surpass this problem, classifiers are often deduced from voxels of an anatomically or functionally defined region-of-interest (ROIs), generating a multivariate brain mapping.

Searchlight Mapping (Kriegeskorte et al. 2006) is a usually used method to discover the discriminative brain regions that should be considered in ROIs definition. Instead of analysing one voxel at a time, this approach performs a joined multivariate analysis of one visited voxel and several voxels in its

neighbourhood. The amount of considered voxels in the so called neighbourhood is defined by the size of a sphere, i.e., a nearby voxel is considered to belong to the visited voxel's neighbourhood if it is located at a certain Euclidean distance (less than or equal to the sphere's radius). The result of the multivariate analysis (the t value resulting from a multivariate statistical comparison) within this sphere is then stored at the visited voxel. By visiting all voxels and analyzing their respective (partially overlapping) neighborhoods, one obtains a whole-brain map that allows the identification of the areas that show patterns of activation capable of providing discriminative information about two or more different tasks from the experimental protocol.

2

Methods

2.1) Data Acquisition

➢ Participants

Functional Magnetic Resonance data was acquired from ten right-handed volunteers, with ages between 24 and 47 (mean age 32,3 ± 8,31 years). All of them had never been diagnosed with psychiatric or neurologic disorders or any kind of chronic condition. Further, none of the ten participants reported to resort to regular medication due to other health problems.

Prior to the acquisition date, the subjects were asked to generate three different written lists, each one containing fifteen groups of two or three words. Two of them had to be filled with words concerning personal past or present and future worries, separately. The third one contained groups of words whose emotional significance is irrelevant to the subject at that time. A feeling-in document with the necessary instructions were delivered to each subject in order to assist and ease their participation. Additionally, participants read and signed a confidential Inform Consent approved by the local ethics committee (Comissão de Ética da Faculdade de Medicina da Universidade de Coimbra), which contained important information about the study's motivation, procedures and its possible benefits and risks.

➢ Task and Experimental Design

The type of fMRI experimental design used is called Blocks design. It is characterized by more extended time intervals for each condition which will lead to a larger evoked response during each task, thus increasing the separation in signal between blocks, ultimately leading to higher detection power.

Once in the MRI Scanner, subjects were confronted with their personal previously written words. Each word appeared for 2s in a screen and the participants were asked to read and reflect about it. Every type of word was separated in three different condition blocks of 30s (neutral, past/present worrying or future worrying), each of which repeated ten times over the course of data acquisition. Intercalated with the conditions blocks, there was also a 30s-lasting resting block during which participants were asked to fixate a cross that appeared in the centre of the screen.

A simplified representation of our block design paradigm is portrayed in Figure 2.1.

Figure 2.1: Representative squeme of the block design paradigm used in the present work. Each block represents the variation across time of the hemodynamic response function during onde specific condition.

➢ MRI Acquisition Parameters

The main acquisition details of anatomical and functional image's acquisition are listed in Table 2.2 and Table 2.3, respectively.

Pulse Sequence	*Eco Planar (EPI)*	***Inplane Y***	*3.04762 mm*
Echo Time	*30 ms*	***Slice Thickness***	*3 mm*
Repetition Time	*2500 ms*	***Gap Thickness***	*0 mm*
MRI Scanner	*Siemens Magneton Trio 3T*	***Interslice time*** $(\frac{TR}{Number\ of\ Slices})$	*65 ms*
Number of Slices	*38*	***Slice Resolution***	*Number of Columns: 84*
Number of Volumes	*725*		*Number of Rows: 84*
Number of Skipped Volumes	*0*	***Mosaic Matrix***	*7 x 7*
Inplane X	*3.04762 mm*	***Slice Scanning Order***	*Interleaved*

Table 2.2: Functional Magnetic Resonance Imaging acquisition parameters

Image Resolution	*Number of columns: 256*	***Slice Thickness***	*1 mm*
	Number of rows: 256	***Spacing Between Slices***	*0 mm*
Pulse Sequence	*MPRAGE*	***Repetition Time***	*2530*
Number of Slices	*176*		

Table 2.1: Anatomical Magnetic Resonance Imaging acquisition parameters

2.2) *Data Processing*

Because both functional and anatomical raw images may not be perfectly aligned (due to subjects' movements) and may exhibit scanning artifacts, simply overlapping them may provide erroneous results. Therefore, both anatomical and functional images must be processed separately before coregistration.

The scheme portrayed in Figure 2.2 shows the various steps taken throughout data processing in this particular work.

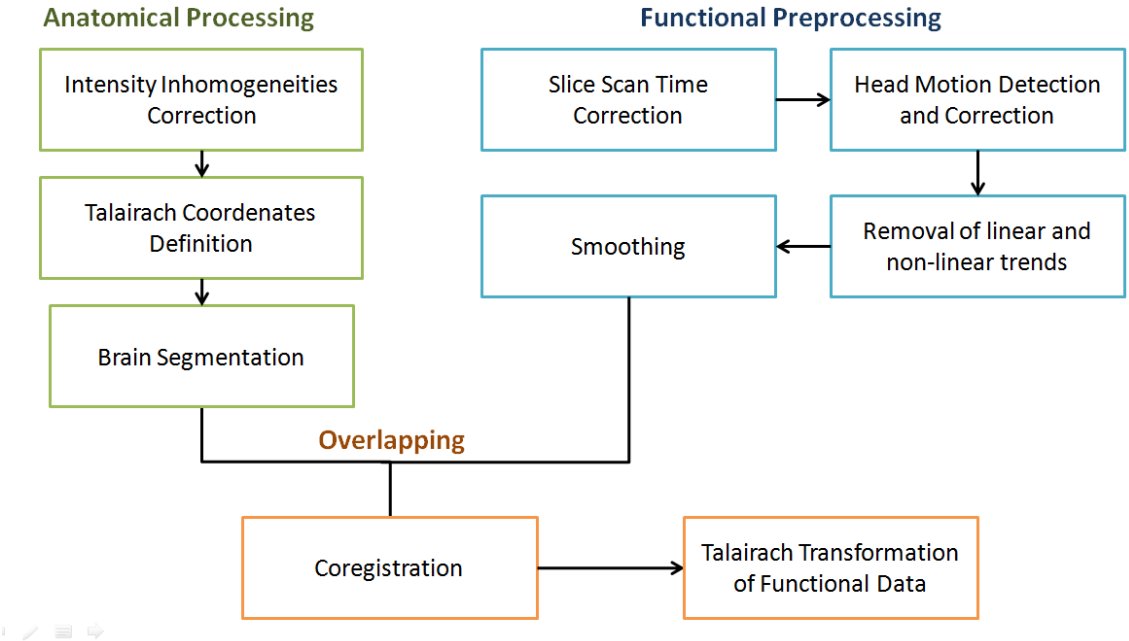

Figure 2.2: Data processing steps arranged in a scheme

All data handling were performed using the software package *BrainVoyagerQX 2.8*. The following described information about the processes and methods to image processing and statistical analysis are featured in *Brainvoyager*'s Support website.

➢ Anatomical Data Processing

Intensity Inhomogeneities Correction

First of all, contrast and brightness were adjusted manually in order to obtain grey matter intensities of approximately "100" and white matter intensities around "160", providing the best grey-white matter separation possible and allowing a proper visualization of the brain cortex.

Since during data scanning the inhomogeneities of the applied magnetic fields may induce artifacts in the acquired anatomical images, the first move in anatomical data processing must be intensity inhomogeneity correction (IIHC). The software offers an automatic tool that executes IIHC without user's intervention. This tool performs image's background cleaning and erosion, detection of white matter and bias field estimation (see detailed steps in Appendix 7) to generate a new 3D anatomical image whose voxels have much more homogeneous intensities (grey matter intensities will be centred around intensity "100" and white matter intensities around "160" by default). IIHC improves anatomical data's visualization and creates better starting points for subsequent segmentation tools.

Talairach Coordenates Definition

Due to anatomical variability across subjects, it is very important to define a common coordinate space in which both structural and functional images can be overlapped. The most commonly used standard space is called the *Talairach* space and is obtained by submitting both anatomical and functional data to a *Talairach* transformation. *Talairach* coordinates are defined directly in the structural data, through manual identification of specific anatomical regions. For more detailed information about *Talairach* transformation see Appendix 6.

Brain Segmentation

Using certain anatomical data processing methods it is also possible to segment and reconstruct the cortex of both hemispheres of the brain. As a result, we obtain a 3D structure representing the anatomical surface of the cortical

mesh. Brain segmentation is essential for volume or surface rendering, as well as for precise estimates of cortical thickness. In the present study, brain segmentation allowed us to build a mask of the cortex which was, posteriorly, used in the multi-voxel pattern analysis technique further discussed (see subchapter 2.5).

BrainVoyager QX provides an automatic cortex segmentation tool, in which a series of steps are sequentially performed until the 3D reconstructed structure is finally delineated (see Appendix 2).

➢ Functional Data Preprocessing

Following anatomical image reconstruction and in order to prepare the statistical analysis, it is important to remove artifacts and confound variability from the acquired functional data. For that, we resort to a series of computational processes that are collectively called preprocessing. *BrainVoyager QX* has in-built functions, however it is important to understand all steps in order to guarantee accurate results.

Slice Scan Time Correction

Slice scan timing correction is applied to eliminate the time-variability between scanned slices (not all brain regions are scanned at the same moment in time) that could lead to suboptimal statistical analysis. To achieve temporal alignment amongst slices, each slice's data is shifted in time from its original scan time point to match the same time point as when a reference slice (the first slice of the functional volume in our case) was acquired (see Appendix 3). With this purpose, the software relies on information from the defined acquisition protocol.

All shifted slices must undergo changes in data in order to better represent the information that would have been recorded if the original time point coincided with the reference. In our study, the estimation of new voxel intensity values was accessed using a *sinc* interpolation. This method offered a better compromise between spent time and results reliability.

Head motion detection and correction

Since the most common artifacts come from subject's head movements within the scanner, *BrainVoyager QX* also counts with a standard optimization algorithm that enables the correction of head movement by coregistrating successive image slices to a single reference one (in this case the first scanned slice) using, once more, a combination of three translations and three rotations (see Appendix 4).

As a final step, to gauge new volume's signal values whose position fall in-between measured data points, we resort to *trilinear sinc* spatial interpolation. This interpolation method achieves the highest quality results, i.e. gives rise to corrected functional volumes that reflect the original data as closely as possible.

Removal of Linear and non-linear trends

Linear and non-linear trends correction is also a very important preprocessing step, since it allows the removal of low-frequency drifts caused normally by physiological noise (heart beat, breathing and others) or physical noise (from the MRI scanner) that would decrease substantially the power of statistical data analysis. These low-frequency drifts are removed through the application of a high-pass filter in each individual voxel's time course. In general, high-pass filters remove low-frequency portions of a signal (the drifts in this case) while preserving the high-frequency ones.

In our study we opted to perform a temporal high-pass filtering using general linear model approach with Fourier basis set (see Appendix 5), which is the most efficient in detecting the signals with the lower frequencies and effectively removing them. The design matrix obtained with the GLM dictates the filter's cut-off value which is usually specified by sine and cosine waves, whose cycles fall within the extent of the fMRI data. In this step of preprocessing fMRI data, two sine/cosine cycles were used.

Spatial and Temporal Smoothing

Temporal and spatial filtering may also be used to perform the smoothing of the acquired image. The advantages of smoothing are: improving of signal-to-noise ratio, reducing high-frequency spatial components and, most importantly, easing group analysis by improving inter-subject registration and overcoming limitations in the spatial normalization by blurring any residual anatomic differences. A mean smoothing filter of 8 mm Full Width Half Maximum was applied to this study's data as the last step of the preprocessing of functional information.

➢ Overlaying Functional and Anatomical data

Coregistration

The coregistration of functional and anatomical data sets is performed automatically by the software, upon previous indication of the chosen strategies. It may be divided in two main steps: an initial alignment (IA) followed by a fine-tuning alignment (FA).

In this study's particular case, since anatomical and functional data are both recorded in the same session and in a file format containing the required positioning information, an IA with resource to header-based coregistration will be performed.

Since IA already assured a considerably close positioning of the two data sets, the role of FA is to perfectly adjust the alignment with resource to iterative minimization techniques. In this case, a FA using Gradient-Driven affine transformations was performed. This strategy is the most powerful FA procedure, since it uses signal intensity changes with respect to neighbouring voxels as a reference measure to evaluate the quality of the alignment. By using intensity gradient instead of intensity per se, this technique ceases to be influenced by inhomogeneities in the recorded data, thus providing more reliable results.

Talairach Transformation of Functional Data

In order to assure a reliable and precise interpretation of the functional results given by coregistration, functional data must also be converted into the *Talairach* space. *BrainVoyager Qx* is able to perform the *Talairach* transformation of the functional data automatically, with resource to several pieces of information produced in previous steps: the preprocessed functional image, both IA and FA alignments of anatomical and functional data, AC-PC translations and rotation performed and cerebrum borders defined. By linking the transformed functional and anatomical data, we obtain an aligned and normalized image containing a 4D data set: 3D space x 1D time.

2.3) Single Study Statistical Analysis

So far we have both anatomical and functional data converted into *Talairach* coordinates system and ready for statistical analysis. The first recomended stage of fMRI statistical analysis encompasses the examination of each subject's data separately, in order to ascertain that all preprocessing stages were successfully implemented.

In our study, we opted to apply a General Linear Model to each subject's preprocessed functional data to create the statistical maps of all brain areas recruited during each one of the different conditions of the experimental paradigm.

➢ The General Linear Model (GLM)

As seen so far, the GLM aims to predict the variation of the observed fMRI time course of a voxel for different conditions with respect to the expected time course of a theoretically idealized hemodynamic response function.

We created a stimulation protocol file for the Block design, using a graphical procedure based on a segmented visual representation of time. The regularly spaced conditions may then be manually marked in this graphic.

BrainVoyager QX automatically identifies the main GLM predictors (three, one for each condition excluding the resting state) using the previously defined protocol. In addition, we introduced six new parameters (generated from the resulting file from 3D motion correction), one for each translational and rotational rigid movement imposed to the functional data during detection and correction of head movements. This will allow controlling for the effect of motion in possible creation of false positives.

In this project, we performed serial correlations correction using BrainVoyager QX's AR(1) process (explained in subchapter 1.6).

Since GLM is performed independently for each voxel's time course, the result of its statistical operations will be a set of estimated beta values attached to each voxel. Resorting to a %-Transform, it was possible to obtain voxel-specific statistical values (t and p) for a specified contrast (comparison between two different tasks from the experimental protocol) using each voxel's vector of betas as an input. The estimated t and p values are then collected in a 3D data set known as statistical map. This map will show the estimated statistical values at the position of each corresponding voxel in the *Talairach* transformed functional data. By establishing specific minimal and maximal thresholds that must be or not exceeded by voxel's functional intensities, respectively, it is possible to overlap the statistical map to a 3D anatomical image and visualize only p and t values of functional voxels with statistical significance while still seeing anatomical information as the background. The final 3D image obtained will show anatomical information in a grey colour scale, and statistically relevant functional information in a multiple colours scale, using red-to-yellow colour range for positive values and a green-to-blue colour range for negative values. Ultimately, it will be possible to analyse and localize with relative precision (due to the fact that both anatomical and statistical map are in the same coordinate system – the *Talairach* space) the brain areas exhibiting significant signal modulations (that were more likely recruited) during a specific task.

2.4) Group-Level Statistical Analysis

➢ Fixed Effects (FFX) Group Analysis with False Discovery Rate (FDR)

In this study, the intersubject analysis was initialized by combining all data points from all subjects into a single analysis, using Fixed Effects Group Analysis. We saw that FFX assumes that the effect of the experimental manipulation is fixed across subjects, with possible differences between subjects caused by random noise.

BrainVoyager QX's multi subject analysis tool uses the previously obtained single study GLM information to automatically concatenate the data from all subjects and create a multi-study design matrix. Using a z-transformation, the discrete values that integrate the new design matrix are then converted into a complex frequency domain function, and the variance between subjects is normalized. As a result, we obtain a volume map that, when overlaid to an anatomical image, can provide information about which brain areas are activated across subjects persistently during a certain task.

The final volume map must be tested for statistical significance using the more appropriate technique. This technique should allow the overcoming of the multiple comparison problems, while providing relevant results. In our case, for such a small number of participants, the Bonferroni approach did not give any results. Therefore, we opted to use the False Discovery Rate technique, with q-values from 0.01 to 0.05 (see Appendix 1).

➢ Random Effects (RFX) Group Analysis with Cluster-Level Statistial Thresholding

For generalizable conclusions, the search for correlations between results from different subjects was taken further, this time resorting to Random Effects Analysis that calculates the variability of the obtained data across subjects.

Usually, RFX operates in two statistical levels: one in which mean effects estimation per condition is performed for each subject; and another which receives the first-level RFX results as independent variables and models their variability across subjects.

In *Brainvoyager QX*, RFX's first-level results are a GLM outcome, namely the set of estimated effects (β values) for each subject undergoing one specific condition. These results are then subjected to one second-level statistical analysis method. In our case, we chose to perform an RFX-GLM which operates substantially faster than any other method, and requires much less working memory. With RFX-GLM, a summary statistics approach receives the first-level GLM beta values as input and specifies the same contrast across them, calculating this contrast's mean value and testing it against zero using a t-test.

Since throughout the RFX-GLM approach the majority of the data was examined separately for each subject, the volume map resulting from this stage of the statistical analysis can be generalized to the population.

Finally, the resulting volume map was tested for statistical significance with a Cluster-Level Thresholding (see Appendix 1). In order to find the appropriate cluster size, *BrainVoyager QX*'s Cluster-Level Statistical Threshold Estimator plug-in, the "*ClusterThresh*", was used. *Clusterthresh* iteratively calculates the minimum possible cluster threshold via *MonteCarlo* simulations of the random process of image generation. The number of performed iterations at this point was the recommended by the plug-in creators, i.e. 1000 iterations. The plug-in then estimates spatial correlations between neighbouring voxels and their intensities. Finally it identifies the minimum cluster size threshold, which becomes automatically set in *BrainVoyager QX*'s volume map options.

2.5) Multi-Voxel Pattern Analysis (MVPA)

In *BrainVoyager QX*, MVPA methods are supervised, which means that all classifications are performed with knowledge of the experimental protocol. This fact allows us to assess the generalization performance of a classifier, since the

classification of each activation pattern is already known. Thus, some cases of poor generalization performance due to overfitting (the condition of the mapping function are overly adjusted to the learning set) may be detected.

- **Trial Estimation**

The training map functions (the conjunction of all feature vectors) for each class is created using a standard GLM whose beta values are estimated (resorting to a 2gamma HRF) for each individual trial. As seen previously, the beta values represent the amplitude of the hemodynamic response of relevant voxels at a certain time point. The trial estimation step allows the obtainment of as many training exemplars as possible for each class, by using the estimated betas for each trial per voxel as the trial response values that will integrate the feature vectors.

- **Searchlight Mapping**

In the present study, we performed whole-brain multivariate searchlight mapping. The implemented multivariate statistic method to estimate the t-value of each voxel was a Support Vector Machine based (SVM) searchlight with a sphere radius of 2 voxels. Additionally, we created a mask of the cortex to confine the search of pattern of activity to grey matter

In both multivariate statistical estimation methods, the activity patterns were examined for two experimental conditions at a time (past and future, past and neutral or future and neutral words).

The results were obtained using a two-fold cross validation technique instead of just choosing which trials would constitute training or test components, thus ensuring more accurate and unbiased results. In this technique, training data is divided into several "folds" which are, then, used one by one as testing sets.

3

Results

The main outcomes of this study were obtained with resort to *BrainVoyager QX* package, version 2.8.

In this chapter, we put forth the more relevant imaging results obtained in the present study. RFX, FFX and MVPA results will also be summarized in three tables containing the *Talairach* coordinates of the voxel with greatest t-value in every single cluster of brain activation or deactivation detected. These tables will also provide information about the anatomical nomenclature of each recruited brain region, obtained with resort to *Talairach Client* (Lancaster et al. (1997) and (2000)). This component of the *Talairach Software* (available online) reports *Talairach* labels for user-defined coordinates.

3.1) Group-Level Results

Only the relevant imaging results obtained with RFX will be presented (since they are the ones that can be effectively generalized to the population). The FFX results will only be portrayed in the respective *Talairach* table.

➢ Imaging Data from RFX Group-Level Analysis

Brain Areas Recruited for Past Condition > Neutral Condition

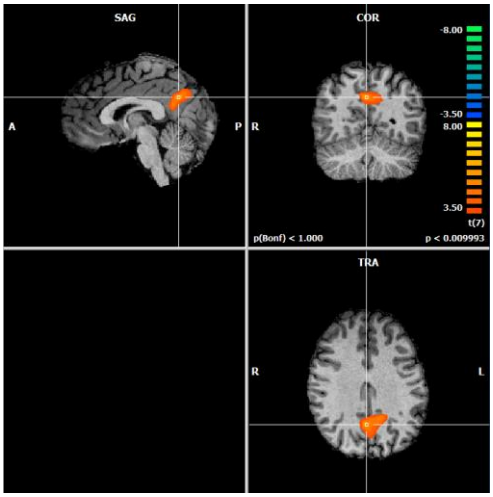

Figure 3.3: RFX Results. Relevant recruitment of precuneus (BA 7) for Past Condition > Neutral Condition

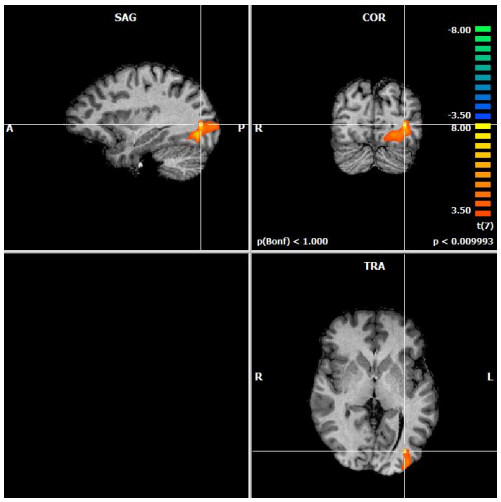

Figure 3.4: RFX Results. Relevant recruitment of middle occipital gyrus (BA 18) for Past Condition > Neutral Condition

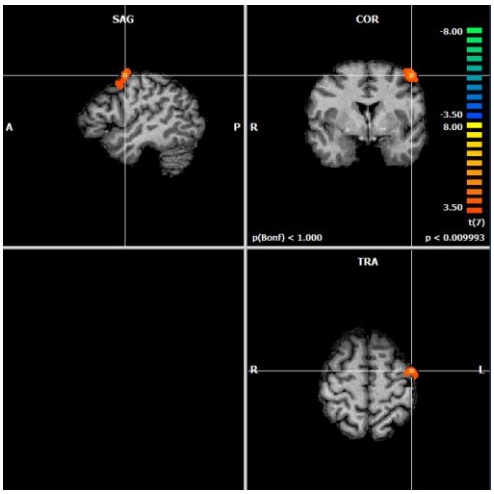

Figure 3.2: RFX Results. Relevant recruitment of precentral gyrus (BA 6) for Past Condition > Neutral Condition

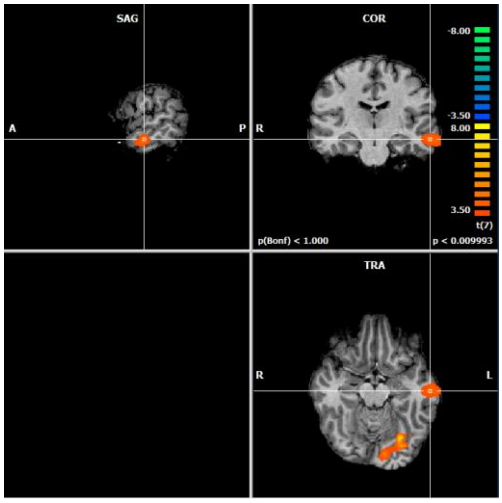

Figure 3.1: RFX Results. Relevant recruitment of middle temporal gyrus (BA 21) for Past Condition > Neutral Condition

Brain Areas Recruited for Neutral Condition > Future Condition

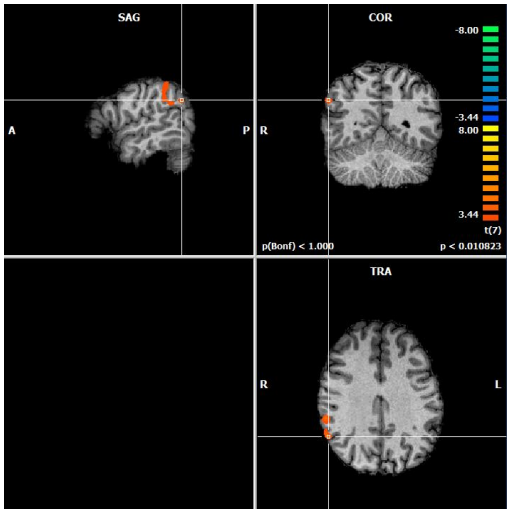

Figure 3.5: RFX results. Relevant Recruitment of supramarginal gyrus (BA 40) for Neutral Condition > Future Condition

Brain Areas Recruited for Past Condition > Future Condition

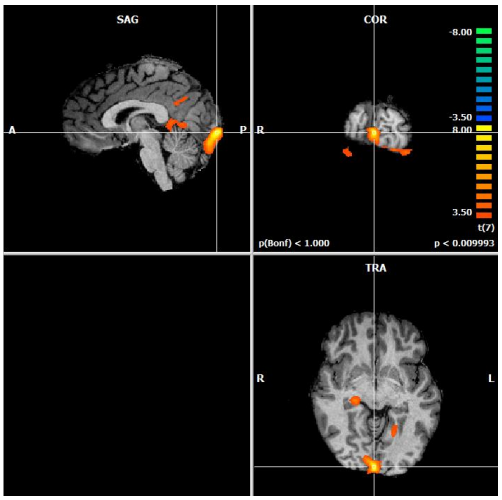

Figure 3.6: RFX results. Relevant Recruitment of primary visual cortex (BA 17) for Past Condition > Future Condition

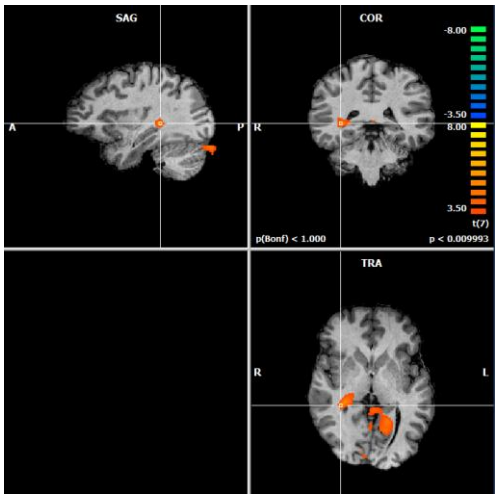

Figure 3.7: RFX results. Relevant Recruitment of the caudate tail for Past Condition > Future Condition

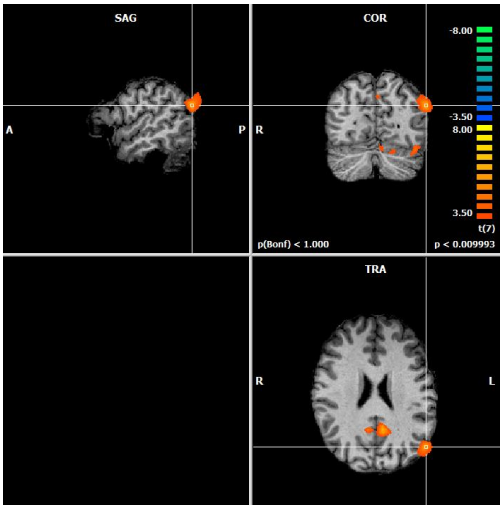

Figure 3.8: RFX results. Relevant Recruitment of middle temporal gyrus (BA 39) for Past Condition > Future Condition

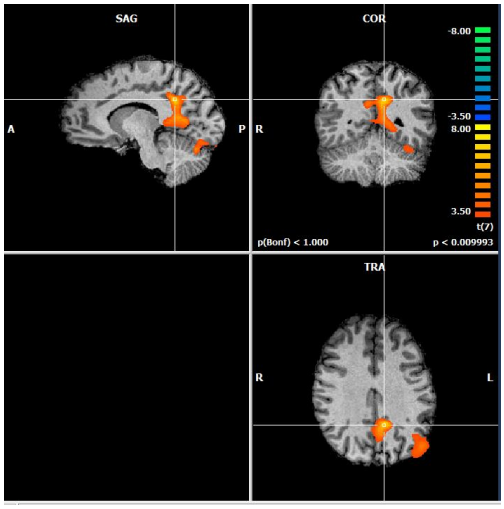

Figure 3.9: RFX results. Relevant Recruitment of precuneus (BA 31) for Past Condition > Future Condition

Brain Areas Recruited for Past and Future Conditions > Neutral Condition

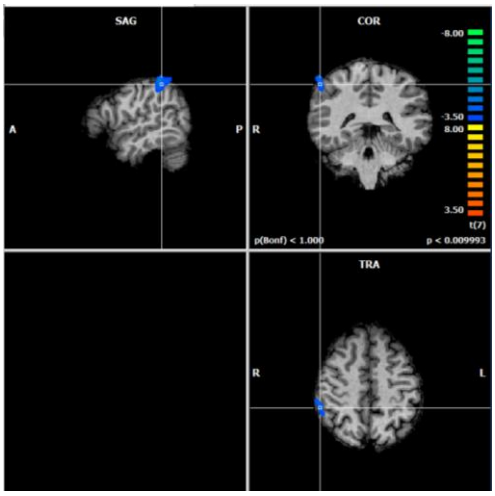

Figure 3.10: RFX results. Relevant Recruitment of parietal lobule (BA 40) for Past and Future Conditions > Neutral Condition

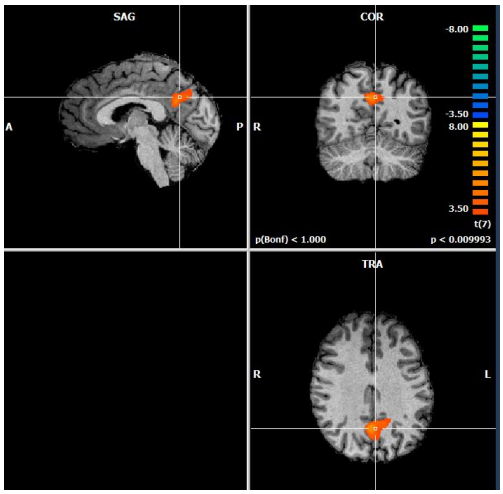

Figure 3.11 RFX results. Relevant Recruitment of precuneus (BA 7) for Past and Future Conditions > Neutral Condition

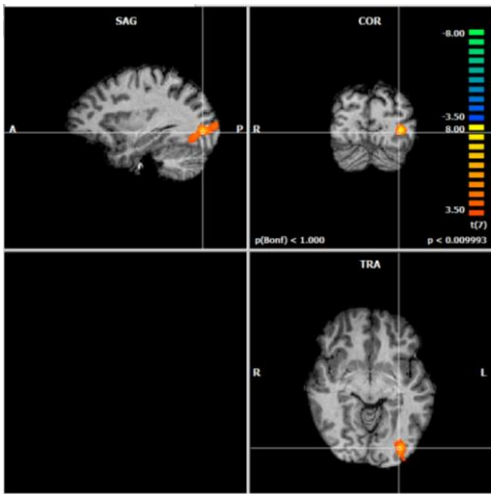

Figure 3.12: RFX results. Relevant Recruitment of middle occipital gyrus (BA 18) for Past and Future Conditions > Neutral Condition

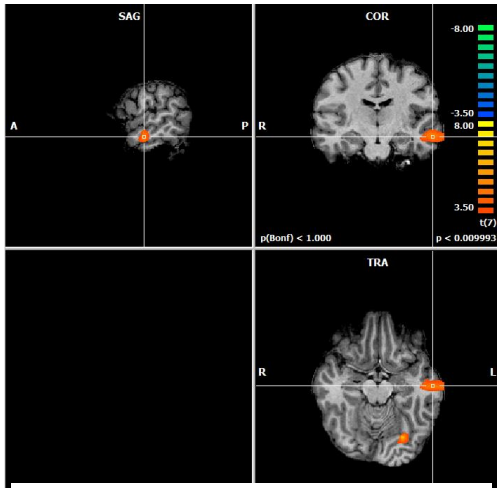

gure 3.13: RFX results. Relevant Recruitment of middle temporal gyrus (BA 21) for Past and Future Conditions > Neutral Condition

➢ RFX Talairach Coordinates Table

Contrast	Brain Region	Brodmann Area	Talairach Coordinates			t-value	p-value	Considered Cluster Thresholds
			x	y	z			
Reading past WI words > reading N words	Right Cerebrum, Parietal Lobe, Precuneus	BA 7	2	-56	30	5,757444	<0,000693	75 voxels
	Left Cerebrum, Occipital Lobe, Middle Occipital Gyrus	BA 18	-31	-77	3	9,12903	<0,000039	75 voxels
	Left Cerebrum, Frontal Lobe, Precentral Gyrus	BA 6	-46	-2	54	5,104685	<0,001392	75 voxels
	Left Cerebrum, Temporal Lobe, Middle Temporal Gyrus	BA 21	-58	-17	-12	5,73409	<0,000710	75 voxels
Reading N words > reading future WI words	Right Cerebrum, Parietal Lobe, Supramarginal Gyrus	BA 40	53	-53	30	5,877501	<0,000613	63 voxels
Reading past WI words > future WI words	Right Cerebrum, Occipital Lobe, Lingual Gyrus	BA 17 (Primary Visual Cortex (V1))	2	-92	-3	9,039369	<0,000041	64 voxels
	Right Cerebrum, Temporal Lobe, Caudate	Caudate Tail	32	-35	3	5,877501	<0,000613	64 voxels
	Left Cerebrum, Parietal Lobe, Precuneus	BA 31	-10	-50	30	7,237405	<0,000172	64 voxels
	Left Cerebrum, Temporal Lobe, Middle Temporal Gyrus	BA 39	-52	-68	24	10,33491	<0,000017	64 voxels

Reading past and future WI words > reading N words	Right Cerebrum, Parietal Lobe, Inferior Parietal Lobule	BA 40	53	-35	51	-5.965890	<0.000561	50 voxels
	Right Cerebrum, Parietal Lobe, Precuneus	BA 7	2	-56	30	5.874384	<0.000615	50 voxels
	Left Cerebrum, Occipital Lobe, Middle Occipital Gyrus	BA 18	-31	-80	0	8.883090	<0.000046	50 voxels
	Left Cerebrum, Temporal Lobe, Middle Temporal Gyrus	BA 21	-55	-17	-9	5.279329	<0.001149	50 voxels

BA, Brodmann Area; WI, worry-inducing; N, neutral

Table 3.1: RFX Talairach Coordinates Table with t-values, p-values and cluster threshold for multiple comparisons correction

➢ FFX Talairach Coordinates Table

Contrast	**Brain Region**	**Brodmann Area**	**Talairach Coordinates**			**t-value**	**p-value**	**FDR q-value**
			x	y	z			
Reading past WI words > reading N words	Right Cerebrum, Parietal Lobe, Inferior Parietal Lobule	BA 40	50	47	45	-4,473007	<0,000008	<0.010
	Right Cerebrum, Occipital Lobe, Lingual Gyrus	BA 17	11	-89	3	4,542227	<0,000006	<0.010
	Right Cerebellum, Posterior Lobe, Declive of Vermis	-	2	-71	21	4,217077	<0,000025	<0.010
	Left Cerebrum, Frontal Lobe, Superior Frontal Gyrus	BA 10	-19	61	27	5,780389	<0,000000	<0.010
	Left Cerebrum, Limbic Lobe, Cingulate Gyrus	BA 31	-7	-53	30	5,965476	<0,000000	<0.010
	Left Cerebrum, Sublobar, Caudate	Caudade Head	-4	1	3	4,808735	<0,000002	<0.010
	Left Cerebrum, Frontal Lobe, Medial Frontal Gyrus	BA 6	-7	4	54	4,649238	<0,000003	<0.010
	Left Cerebrum, Occipital Lobe, Lingual Gyrus	BA 18	-10	-86	-6	4,21794	<0,000026	<0.010
	Left Cerebrum, Limbic Lobe, Anterior Cingulate	BA 32	-10	37	24	4,353224	<0,000014	<0.010

	Left Cerebrum, Frontal Lobe, Superior Frontal Gyrus	BA 8	-16	40	48	4,601318	<0,000004	<0.010
	Left Cerebrum, Sublobar, Claustrum	-	-25	25	12	4,309097	<0,000017	<0.010
	Left Cerebrum, Frontal Lobe, Inferior Frontal Gyrus	BA 46	-49	28	0	5,238073	<0,000000	<0.010
Reading N words > reading future WI words	Right Cerebrum, Parietal Lobe, Inferior Parietal Lobule	BA 40	50	-50	42	4,008603	<0,000062	<0.050
	Right Cerebrum, Frontal Lobe, Middle Frontal Gyrus	BA 6	41	10	48	4,523876	<0,000006	<0.050
	Right Cerebrum, Frontal Lobe, Superior Frontal Gyrus	BA 10	41	52	27	4,537495	<0,000006	<0.050
	Right Cerebrum, Frontal Lobe, Middle Frontal Gyrus	BA 10	35	55	0	4,393353	<0,000011	<0.050
	Left Cerebrum, Frontal Lobe, Inferior Frontal Gyrus	BA 47	-49	29	-1	-4,257	<0,000021	<0.050
Reading past WI words > reading future WI words	Left Cerebrum, Frontal Lobe, Inferior Frontal Gyrus	BA 47	-33	28	-12	4,939	<8,0201e-07	<0.050
	Left Cerebrum, Limbic Lobe, Posterior Cingulate	BA 29	-7	-50	9	4,690795	<0,000003	<0.050
	Left Cerebrum, Frontal Lobe, Inferior Frontal Gyrus	BA 47	-34	28	-12	5,068107	<0,000000	<0.050
	Left Cerebrum, Limbic Lobe, Posterior Cingulate	BA 29	-7	-50	9	4,691	<0,000003	<0.050
	Right Cerebrum, Sublobar, Thalamus	-	20	-24	-3	4,214	<0,000025	<0.050
	Right Cerebellum, Posterior Lobe, Inferior Semi-Lunar Lobule	-	47	-62	-36	4,657521	<0,000003	<0.050
Reading past and future WI words > reading N words	Right Cerebrum, Parietal Lobe, Inferior Parietal Lobule	BA 40	50	-47	42	-4.789233	<0.000002	<0.030

	Right Cerebrum, Frontal Lobe, Middle Frontal Gyrus	BA 8	35	28	42	-4.217663	<0.000025	<0.030
	Right Cerebrum, Frontal Lobe, Superior Frontal Gyrus	BA 10	41	52	27	-4.017667	<0.000059	<0.030
	Right Cerebrum, Frontal Lobe, Superior Frontal Gyrus	BA 10	32	55	0	-4.417354	<0.000010	<0.030
	Right Cerebrum, Occipital Lobe, Cuneus	BA 17	14	-89	3	3.953661	<0.000078	<0.030
	Left Cerebrum, Limbic Lobe, Cingulate Gyrus	BA 31	-7	-53	27	4.804190	<0.000002	<0.030
	Left Cerebrum, Sublobar, Caudate	-	-4	1	3	4.585382	<0.000005	<0.030
	Left Cerebrum, Frontal Lobe, Medial Frontal Gyrus	BA 10	-7	43	-9	4.411681	<0.000010	<0.030
	Left Cerebrum, Frontal Lobe, Medial Frontal Gyrus	BA 6	-7	1	57	4.515027	<0.000006	<0.030
	Left Cerebrum, Frontal Lobe, Superior Frontal Gyrus	BA 10	-16	61	27	4.821038	<0.000001	<0.030
	Left Cerebrum, Frontal Lobe, Inferior Frontal Gyrus	BA 47	-49	28	0	5.607722	<0.000000	<0.030
	Left Cerebrum, Frontal Lobe, Precentral Gyrus	BA 6	-46	-5	54	5.302277	<0.000000	<0.030
	Left Cerebrum, Temporal Lobe, Superior Temporal Gyrus	BA 38	-49	13	-21	4.045871	<0.000053	<0.030
	Left Cerebrum, Temporal Lobe, Middle Temporal Gyrus	BA 21	-52	-14	-12	4.575775	<0.000005	<0.030
	Left Cerebrum, Parietal Lobe, Inferior Parietal Lobule	BA 40	-55	-50	42	-4.067492	<0.000048	<0.030

BA, Brodmann Area; WI, worry-inducing; N, neutral

Table 3.2: FFX Talairach Coordinates Table with t-values, p-values and q(FDR) value for multiple comparisons correction

3.2) Multi-Voxel Pattern Results

➢ Imaging Results from MVPA Searchlight Mapping

Patterns of differentiation between the Past Condition and the Neutral Condition

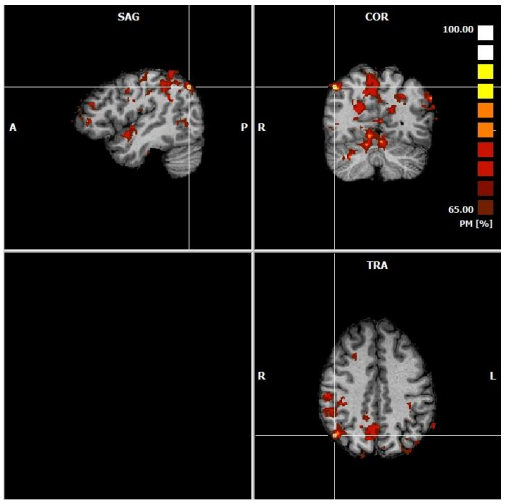

Figure 3.14: MVPA Results. The inferior parietal lobule (BA 39) as a pattern of differentiation between Neutral and Past conditions

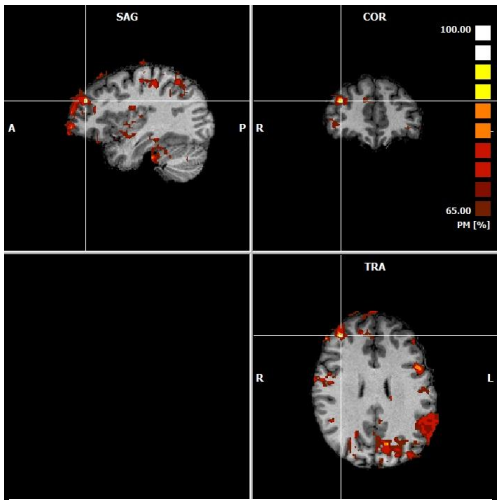

Figure 3.15: MVPA Results. The middle frontal gyrus (BA 9) as a pattern of differentiation between Neutral and Past conditions

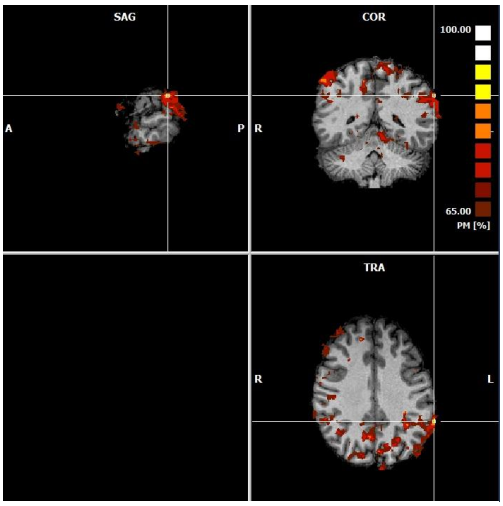

Figure 3.16: MVPA Results. The supramargynal gyrus (BA 40) as a pattern of differentiation between Neutral and Past conditions

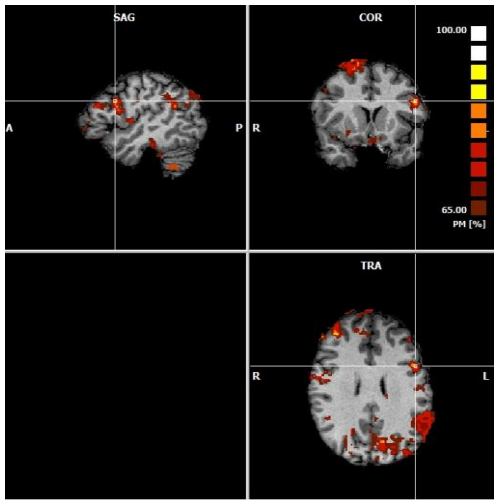

Figure 3.17: MVPA Results. The inferior frontal gyrus (BA 9) as a pattern of differentiation between Neutral and Past conditions

Patterns of differentiation between the Future Condition and the Neutral Condition

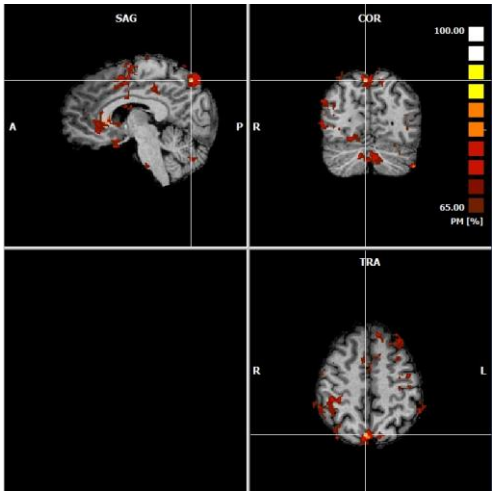

Figure 3.18: MVPA Results. The precuneus (BA 7) as a pattern of differentiation between Neutral and Future conditions

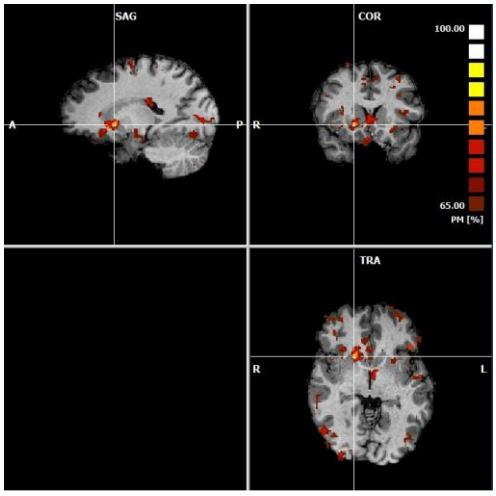

Figure 3.19: MVPA Results. The caudate body as a pattern of differentiation between Neutral and Future conditions

Patterns of differentiation between the Future Condition and the Past Condition

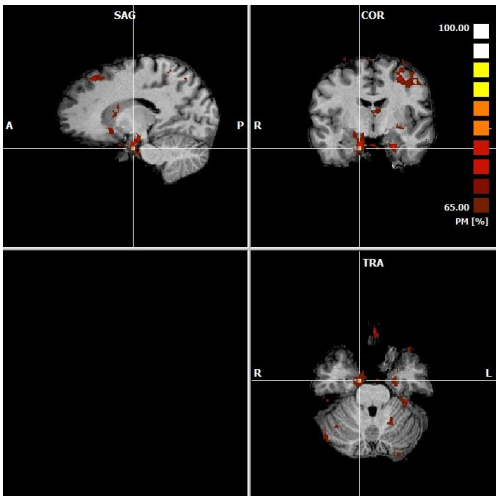

Figure 3.20: MVPA Results. The uncus (BA 34) as a pattern of differentiation between Past and Future conditions

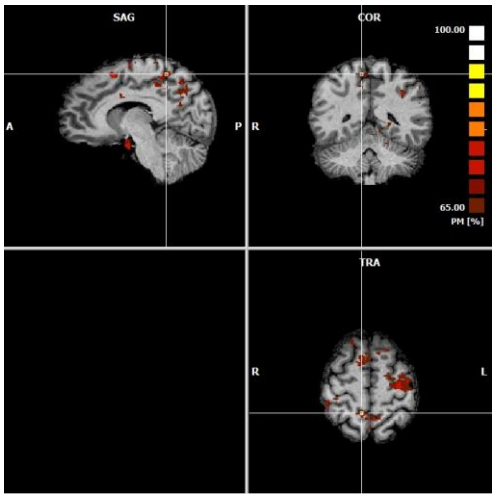

Figure 3.21: MVPA Results. The paracentral lobule (BA 5) as a pattern of differentiation between Past and Future conditions

➢ MVPA Talairach Coordinates Table

Differentiated Conditions	Brain Region	Brodmann Area	Talairach Coordinates			PM
			x	y	z	
Neutral and Future	Right Cerebrum, Parietal Lobe, Precuneus	BA 7	5	-68	48	90.000000 %
	Right Cerebrum, Sublobar, Caudate	Caudate Body	17	13	6	90.000000%
Neutral and Past	Right Cerebrum, Parietal Lobe, Inferior Parietal Lobule	BA 39	44	-62	41	94.999992%
	Right Cerebrum, Frontal Lobe, Middle Frontal Gyrus	BA 9	35	43	27	90.000000%
	Left Cerebrum, Parietal Lobe, Supramarginal Gyrus	BA 40	-61	-44	33	95.000000%
	Left Cerebrum, Frontal Lobe, Inferior Frontal Gyrus	BA 9	-46	10	27	90.000000%
Past and Future	Right Cerebrum, Limbic Lobe, Uncus	BA 34	14	-8	-24	90.000000%
	Right Cerebrum, Frontal Lobe, Paracentral Lobule	BA 5	8	-44	54	90.000000%

BA, Brodmann Area

Table 3.3: Multi-Voxel Searchligh Mapping results and respective percent accuracy (PM) values

4
Discussion

The present work's main motive was to find the brain areas whose recruitment is related to worrying about past episodes and possible future events of personal relevance to each participant. The obtained results indicate prevalence in brain activation during reading words related to past worries when compared to words related to future worries or neutral words.

The group level analysis results that may be applicable at a population level (RFX results) showed that reading and worrying about personal past episodes involves greater activation than reading neutral words contents, in brain areas such as the medial posterior parietal cortex, left posterior occipital and frontal cortices and left central temporal cortex. Additionally, significant activations in medial posterior occipital and parietal lobe and left posterior temporal lobe were also detected when subjects thought about past negative events when compared with possible negative outcomes of a future situation. On the other hand, worrying about a future incident seemed to encounter less activation of right posterior parietal lobe when compared with neutral content. Finally, worry (past and future) in comparison with neutral thinking, were characterized by activation of the medial posterior parietal cortex, left posterior occipital lobe and left central temporal lobe, as well as deactivation of right dorsal-posterior parietal cortex.

Functional information about each specific recruited area during all the performed contrasts between conditions will be further discussed in the following subchapters.

4.1) Functional Description of the Relevant Recruited Brain Areas

➢ Recollection of Past negative events and imagining Neutral entities

Overall there was higher brain activation when subjects were asked to read and think about their personal past worry-inducing words (past condition) than when they read on neutral entities (neutral condition).

During past condition, the group-level data analysis with resort to RFX-GLM set forth activation in precuneus (BA 7) and middle occipital (BA 18), precentral (BA 6) and anterior middle temporal (BA 21) gyri.

Precuneus is a medial posterior part of the parietal cortex, whose anatomical and functional connections are thought to be rich and to widespread across various brain regions (Zhang et al. (2011); Jones et al. (2013)). Its activation during the past condition was, somehow, expected, since it seems to be involved in mental imagery, self-referential thinking, episodic memory retrieval (Zhang et al. (2011); Jones et al. (2013)) and regeneration of episodic contextual associations (Lundstrom et al. (2005)).

Much like ventral precuneus, the middle occipital gyrus seems to be involved in recognition of meaningful sentences and retrieval of word-pairs (Zhang et al. (2011)). Its more significant activation during the past task suggests that the way we process semantic information is dependent of its content. Furthermore, as have been seen before, BA 18 encompasses the secondary visual cortex (particularly V2) which is thought to be involved in the construction of an event's mental imagery (Addis et al. (2007)). One possible interpretation of V2 recruitment during the past condition may be the existence of more engaging mental imagery while worrying about past episodes in comparison with the neutral task.

Brodmann area 6, probably the largest area, covers part of the precentral gyrus and is situated in premotor cortex which plays an important role in controlling physical movements. Moreover, the premotor cortex shows high connectivity with secondary motor areas such as the supplementary motor cortex (SMA) which is also covered by BA 6. Although SMA were not recruited in our results, this connectivity may prove to be interesting in the context of the present work, since SMA is thought to be involved in motor imagery of locomotor-related tasks (Malouin et al. (2003)).

A growing body of literature suggests that the middle temporal gyrus, especially in the left hemisphere, is implicated in semantic processing such as activation and representation of word meanings (Jung-Beeman et al. (2005); Westerlund et al. (2014)). The continuous activation of this area throughout almost the entirety of our results seems coherent with this fact, seeing that subjects were asked to read words and mentally represent their meaning in every single experimental task.

All mentioned recruited areas were present in the revised literature, with exception of the premotor cortex (BA 6). Although somehow unexpected, it is possible to foresee the reason why this area experienced relevant activation, especially if we consider that imagining certain episodes could encounter mental simulation of one's movements in it.

Some additional brain regions, whose statistical significance is not enough to guarantee a relevant impact across subjects, were identified as being activated (using FFX analysis) during the past condition as opposed to the neutral condition. Of note, the left cingulate gyrus (BA 31).

Cerebral cytoarchitectonic studies often divide the cingulate cortex in three main areas. The portion including Brodmann area 31 is considered part of the posterior cingulate cortex (PCC), which has been robustly studied in the past years due to its activation during emotional stimuli (Maddock et al. (2002)). PCC is thought to undergo activation in healthy humans when they are retrieving memories from their episodic and autobiographic memory (Maddock et al. (1997)). In fact, PCC were identified as being a key part of the default mode network (Jin et al. (2012)), which appears to be associated with retrieval and manipulation of episodic memories, self-referential processing and pro-

spective memory (Kim et al. (2012)). The mentioned PCC functions emphasize its potential involvement in one's recalling of personal and emotionally arousing episodes that have already occurred, thus proving its activation to be in context with the present study.

- **Envisioning Future Worrying episodes and imagining Neutral entities**

The neutral condition proved to have more activation of the supramarginal gyrus (BA 40) when compared with the future condition. The supramarginal gyrus is thought to underlie phonological processing (i.e. comprehension of speech whether spoken or written) as well as recognition of words resorting to the verbal working memory (Deschamps et al. (2013)). Although this region's activation was not foreseen by the reviewed body of literature, it may suggest that, during the neutral condition, verbal working memory may have been enhanced in juxtaposition to interaction of emotional and memory-related processes that prevails in past and future conditions.

Once more, FFX's high sensitivity may reveal potential false negative RFX results, which could be further tested by increasing sample size. For instance, resorting to FFX, we were able to find one brain area that experienced greater activation during the future condition in comparison with the neutral condition, and was in accordance with the previewed literature: the inferior frontal gyrus (BA 47). In some studies, this brain area is more commonly associated with semantic processing (Grindrod et al. (2008); Tsujii et al. (2011); Liakakis et al. (2011)), contributing in some aspects for processing of word meaning, retrieving and manipulation of semantic knowledge in deductive reason (Tsujii et al. (2011)) or in selection of particular meaning of ambiguous words (Grindrod et al. (2008)). Moreover, Liakakis et al. (2011) studied the diversity of the inferior frontal gyrus to realize it may also be associated with working and episodic memory retrieval. Besides BA 47, the inferior frontal gyrus also covers part of BA 9, which is concerned with more executive and cognitive functions

such as controling automatic behavior (Kübler et al. (2006)) and processing emotional stimuli (Bermpohl et al. (2006)).

- **Envisioning Future Worrying episodes and Recollection of Past negative events**

Our results point towards the existence of greater brain activation during the past condition than in the future condition. The revised literature did not encounter any of the brain areas whose activation were, in our study, identified as being more significant during recollection of past negative-weighted situation than during worrying about prospective events. These areas are: V1 (BA 17), the tail of the caudate nucleus, precuneus (BA 31) and middle temporal gyrus (BA 39).

Besides the precuneus and the middle temporal gyrus, whose thought functions were already described, the the primary visual cortex (V1, BA 17), also showed relatively intenser activation in the past task. Several studies have reported the involvement of V1 in attention, particularly in redirecting attention across space (Posner et al. (1999), Ress et al (2000), Silver et al. (2006)). The maintenance of attention, even during the absence of visual stimulus, was also characterize by sustainment of V1 activity, thus suggesting a correlation between primary visual cortex activation and allocation of visuospatial attention (Ciaramitaro et al. (2007)). Additionally, Ress et al (2000) showed that quantitatively higher activity of V1 originates greater performance in cognitive tasks, which may suggest a positive correlation between V1 activation and the engaged level of attention. In this case, the prevalence of V1 activation during the past condition may suggest that there is a tendency to focus more strongly while remembering negative events from one's past than during envisioning of threatening future episodes one may come across.

Another recruited area was the posterior caudate, also known as caudate tail. The caudate is thought to underlie a great variety of cognitive processes, particularly in expectation of particular contingencies after goal-directed actions (Grahn et al. (2008)). Furthermore, caudate's tail (its most ventral and pos-

terior part) has been implicated in goal-directed learning (Seger et al. (2005); Grahn et al. (2008)), being more recruited by subjects with better performance in learning tasks (Seger et al. (2005)). We hypothesize that the current activation pattern relates mostly to perceptual processes.

Additionally, FFX revealed relevantly greater activation of the posterior cingulate in the past condition in comparison with the future condition. As mentioned before, PCC is thought to be involved in emotion-related processing of not valence-specific (i.e. for both negative and positive valenced emotions) stimuli (Maddock et al. (2002)). The greater activation of this particular area during the past condition when compared to future worrying is in line with the previously mention hypothesis put forth by Botzung et al (2008): thinking about past events encompasses deeper emotion involvement than imagining future events.Additionally, it is worth mentioning that, though not generalizable at a population level, thinking about past unpleasant occurrences may involve more intense manipulation and usage of the autobiographical and episodic memory systems than worrying about the future. This hypothesis represents an unconformity regarding some of the previously mentioned literature whose results were the exact opposite. In fact, the majority of the revised literature about remembering past events and envisioning upcoming prospects suggested that there was greater cerebral activity during future imagining than during past recollection.

- **Worrying thoughts and Imagining Neutral entities**

The brain areas that showed higher activation with worrying rather than non-worrying thoughts (with statistical significance throughout RFX-GLM analysis), independently of their time-stamp, were the precuneus (BA 7), the middle occipital gyrus (BA 18), and the middle temporal gyrus (BA 21).

As previously mentioned, activation of the middle temporal gyrus may be related to semantic processing and words' meaning. The previously referred supramarginal gyrus' greater activation during neutral tasks led us to hypothesize the neutral condition required more working memory assessment and

greater amount of effort in word recognition. On the other hand, the middle temporal gyrus greater recruitment during worrying tasks suggests that word processing and mental representation engage more cerebral activation when subjects were confronted with the emotional worrying sentences as opposed to the neutral ones.

As previously described, the middle occipital gyrus functionalities are tightly linked with recognition of sentences' meaning, while BA 18 is mainly a visual area (V2) responsible for building mental representation of events. If that is the case, middle occipital gyrus activation may constitute more evidence to the supposition that reading and thinking about neutral concepts encounter less semantic procession and less engaging mental imagery than reading and reflecting about personal meaningful words.

The middle occipital and temporal gyri were mentioned by the revised literature; however, they were referred to as being less active during worrying and rumination than during neutral tasks, which was not verified in this case.

Only the inferior parietal lobule (BA 40) appears to undergo more activation associated with the neutral condition. This association area is normally involved in intermodal integration during various cognitive functions (Nishitani et al. (1998); Greene et al. (2010)). Particularly, Brodmann's area 40 concerns the anterior inferior parietal lobule which is thought to be part of brain's default mode network. Inferior parietal lobule's activation during neutral tasks corroborates de hypothesis than, even when thinking about meaningless concepts, we tend to engage in self-referential thoughts.

The results with FFX revealed activation of the left superior (BA 10), middle (BA 6) and inferior (BA 47) frontal gyri, as it was previewed by the literature. Regions of the frontal lobe, in general, are responsible for flexible and adaptative behaviour, and for highly developed social skills (Aminoff and colleagues' Encyclopedia of the neurological sciences, 2nd edition, 2014, pg 358-365).

The superior frontal gyrus is thought to be correlated with the cognitive control network, which is involved in conflict monitoring, error detection, response selection and attention control (Li et al. (2013)). However, what appears to link the superior frontal gyrus to our experimental conditions is its involve-

ment in self-referential processing, which is thought to be highly associated with worrying and rumination.

On the other hand, middle temporal gyrus' functions seem to correlate more with the consciousness of a union or relation between two different events (Carter et al. (2005)). In our context, this feature may be important while constructing mental episodes by associating different pieces of information from one's episodic memory.

Finally, as have been previously mentioned, the inferior frontal gyrus is mainly implicated in semantic processing and retrieving information from working and episodic memory networks.

4.2) Multi-Voxel Patterns of Activation

The searchlight approach to multi-voxel pattern analysis used in our study provided some interesting results.

Patterns of distinction between neutral and past conditions were mainly located in the parietal and frontal lobes. These areas are related to self-referential thought (inferior parietal lobule, BA 39), word identification and processing (supramarginal gyrus, BA 40), identification of related events (middle frontal gyrus, BA 9) and processing emotional stimuli (inferior frontal gyrus, BA 9), thus covering the entire process from simply reading and processing the written words until their mental representation and possible thoughts associated. Roughly the same results were observed in contrasting patterns between the neutral and future conditions: mental imagery, self-referential thinking, episodic memory retrieval (precuneus) and guided outcome-oriented behaviour (body of the caudate). In fact, as suggested by the group-level cerebral activation results, there appears to exist a distinct difference between the way we respond to reading and thinking about neutral entities as opposed to reading and elaborating about time-unrelated personal negative events.

The main brain regions whose activation during past condition were different from future condition were in the limbic (uncus) and frontal (paracentral lobule) lobes. Since the limbic lobe is concerned with emotions, and was, in

general, more activated during the past condition, its distinct activation across past and future tasks constitutes an additional evidence to the hypothesis (put forth by Botzung et al. (2008)) that reflecting about an personally experienced situation encompasses more details, thoughts and feelings associated than envisioning some future event. On the other hand, paracentral lobule constitutes part of the superior parietal lobule which is thought to be involved in manipulation and rearrangement of information within the memory network (Koenigs et al. (2009)). This suggests that, unlike what was proposed by the majority of the revised literature, there are some significant differentiation between the way healthy subjects mentally manipulate memory's information about their past negative and the way possible undesirable future episodes are constructed.

5

Summary / Conclusions

The main aim of the present study was to identify the brain regions recruited while healthy participants read sentences related to personal past episodes and worrying about future events. Amongst the results that may actually be generalized to the control population we verified that recollecting past episodes with negative meaning to oneself yield greater brain activations when compared to both imagining neutral entities and worrying about future situations. This suggests that, as proposed by Botzung et al. (2008), elaborating about experienced negative events possibly involves more active thinking due to the heavier emotional charge it may encounter when compared to imagining possible undesirable outcomes of a situation that has not even occurred yet. In fact, of all three experimental tasks, the one which revealed less brain activation areas associated was the future task, which corroborated this hypothesis.

Our paradigm, in general, revealed the recruitment of brain areas related to self-referential thinking, which suggests that worrying in healthy subjects is associated with internally directed cognition.

In our study, some results are in contraposition to former literature. Henceforth, studies that simultaneously tackle worrying states related to past and future events while reporting results that may be generalizable at the population level are seldom encountered. Attributing a time-stamp to a complex

anxiety state may involve recruitment of many brain areas not taken into consideration in the revised literature.

Furthermore, there are several differences on the whole structure of neurological works that can explain the discrepancy in results between our study and previous studies. For instance, the acquisition parameters, the MRI scanner characteristics and, principally, the experimental paradigm may contribute to different results across researches.

In functional MRI, the conceptualization of how different cortical areas work is anything but straightforward. Logothetis N.K (2012) highlighted that neuronal processes may dominate hemodynamic responses and interfere with BOLD fMRI data. Choosing an experimental protocol that is able to acknowledge and overcome these limitations will, thus, provide more plausible results.

As opposed to the majority of the revised literature, our experimental paradigm was able to provide results not only generalized to the control population, but also significant even after multiple comparison corrections, even though we were handling a relatively small sized sample (only ten people). Therefore, in some ways, our results appear as more robust and consistent. However, the anatomical and functional variability across subjects is always an unavoidable limitation of these type of studies, as well as the complexity in the interpretation of what fMRI activation maps really represent (Logothetis, N.K (2012)).

The construction of a classifier capable of "brain reading" was a complementary part of the present study. The aim was to find a way to roughly identify a worrying-related condition just by analyzing the fMRI data. However, it was not possible to effectuate a profound MVPA analysis owing to the scarce sample of healthy controls considered and, specially, to some unpredictable technical difficulties which could not be resolved on time. Nonetheless, resorting to searchlight mapping, it was possible to identify some differentiation patterns of activation between the considered conditions. These patterns may be used in posterior works as regions-of-interest to be explored with ROI based learning machines (support vector machines, for instance).

6

Future Work

The present work served to delineate the main cerebral activation associated with worrying and, more precisely, with worrying about the past/present or future situations. The implemented experimental paradigm in this fMRI study proved to have a very strong impact since it provided valuable results even with a diminished sample. Consequently, this same paradigm may be used in future studies about worrying and rumination. For instance, studies with insomnia and GAD (generalized anxiety disorder) patients for comparison of the obtained results and possible creation of new diagnostic and treatment methods.

Additionally, since it was not possible to fulfill our expectations regarding MVPA analysis, we propose a further analysis with, possibly, a greater number of participants and, perhaps, even associated to anxiety disorders.

7
Appendix

Appendix 1: Multiple Comparisons Correction Methods in detail

The three most commonly used multiple comparisons correction methods are Bonferroni Correction, False Discovery Rate (FDR) and Cluster-Level Statistical Thresholding.

The Bonferroni correction is the most stringent method of them all. The alpha values estimated by this approach decrease proportionally to the number of the independent statistical tests, as seen in Equation 7.1 (where V is the number of voxels that constitute the fMRI data).

$$\alpha_{bon} = {}^{\alpha}/_{V}$$

Equation 7.1

Although Bonferroni approach effectively improves the false positive rate, it also fails to detect voxels undergoing real activation during a certain studied condition. For many medical and research matters, the loss of truly active voxels is unacceptable and may even be dangerous.

As an alternative, a False Discovery Rate approach has been increasing its popularity. FDR iteratively calculates an alpha value that depends on the distribution of significance values thus allowing the description of the propor-

tion of positive results that are actually false-positives, independently of the number of discovered activated voxels. FDR's actual procedure initiates by ranking the statistical tests (of the V detected activated voxels) according to their uncorrected probability of significance, p (lower probabilities imply greater significance and vice versa), thus obtaining Equation 7.2.

$$p_1 \leq p_2 \leq \cdots \leq p_V$$

Equation 7.2

Then, from the voxel with the smallest probability onwards the algorithm identifies the voxel whose probability index (p_i) is greater than the voxel's ranking in the list (i) divided by the total number of tests (V), as corrected by the desired FDR's q-value (Equation 7.3).

$$p_i = {}^{q_i}/_{V}$$

Equation 7.3

Finally the voxels ranked from p_1 to p_i are considered significant.

FDR's approach for correction of multiple comparisons uses less rigid algorithms than Bonferroni Correction, thus decreasing the false-negatives rate and gaining in experimental power while still being rigorous.

Lastly, a thresholding based on clusters of activation may be alternatively performed. Instead of verifying the significance of the activation of a single isolated voxel, this approach corrects multiple comparisons using information about the activations of several contiguous voxels (clusters of activation). The cluster thresholding method relies on the fact that it is much less likely that a group of very close voxels is activated by chance then that a single isolated voxel turns out to be a false-positive.

Methodologically, in cluster thresholding, the definition of a relatively liberal alpha value (α_C) for voxelwise comparisons is compensated by the gaining in conservatism due to only counting clusters as significant if they are as large as some threshold. As cluster size, C, increases, the number of such clus-

ters (n_C) increases much more slowly than the probability than the given cluster is active. Therefore, the likelihood of a false-positive result decreases with increasing C. The effect of this correlation on the false-positive rate is defined in Equation 7.4.

$$p = (number\ of\ clusterwise\ false - positives) = (1 - \alpha_C)^{n_C}$$

Equation 7.4

Even though the setting of a large threshold may neglect small but meaningful activations, reducing α_C cluster-size thresholding will often reduce the false-negative rate, thus allowing for a more sensitive detection of activated brain regions. However, an important disadvantage goes hand to hand with this technique: it assumes that activation in adjacent voxels is uncorrelated, which is not always true when it comes to fMRI data.

Appendix 2: Brain Segmentation Methods in detail

BrainVoyager QX provides an automatic cortex segmentation tool, in which a series of steps are sequentially performed until the 3D reconstructed structure is finally delineated.

The first step is tissue contrast enhancement: a Gaussian filter with smoothing properties and with the peculiarity of automatically excluding the influence of all neighbouring voxels whose intensities are deviating more than a certain threshold value from the currently considered voxel. This step is crucial to guarantee a better contrast between white and grey matter.

As a second step, the automatic segmentation tools find and fill the brain ventricles. They benefit from the very low intensity signal ("black" voxels) acquired in the ventricle region of T_1-weightened structural MR images, and start a region growing process. The ventricles' area is then filled from one of the detected "black" voxels, through the low intensity neighbouring voxels, until the high intensity boundary voxels. Like the ventricles, other subcortical structures must be identified and labelled as white matter in order to assure that they will not appear as cortical grey/white matter boundaries in the final segmentation. With this purpose, *BrainVoyager QX* offers a *Talairach* mask, created to fit any brain and segment it without removing relevant cortical tissue. Still during the second step, brain surrounding structures' removal also takes place with resource to this software mask.

The following step yields the identification and distinction of brain's grey and white matter. To this end, a series of intensity histograms are built, in which the *X*-axis represent the possible signal intensities, and the *Y*-axis the number of voxels per intensity (frequency). These histograms should show two major peaks, one left-sided and one right-sided, which correspond to the characteristic intensity of grey and white matter, respectively. The software automatically analyses these peaks and suggests an intensity threshold value that separates white from grey matter. This threshold will ultimately allow the tracing and segmentation of the brain meshes of different types of matter in the following steps.

Appendix 3: Slice Scan Time Correction

In slice scan time correction, the rearrangement of individual slices of the functional volume must take into account the order in which they were scanned (slice scanning can be regular or interleaved depending on whether the slices were recorded sequentially or the odd slice numbers were recorded first followed by the even slice numbers, respectively), as portrayed in Figure 7.1.

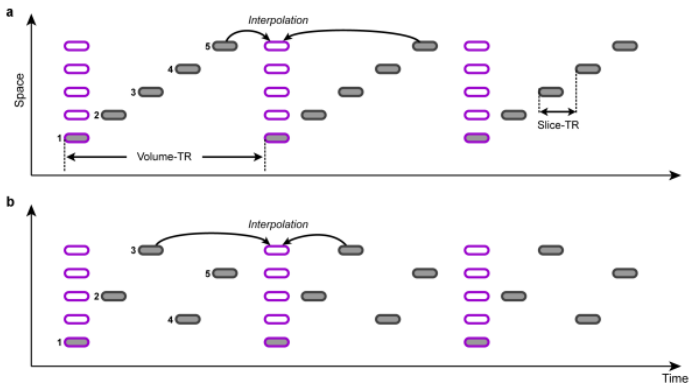

Figure 7.1: Slice shifting during Slice Scan Time Correction for slices that were acquired sequencially (a) and interchangeably (b). (image collected from BrainVoyager's User Guide)

All shifted slices must undergo changes in data in order to better represent the information that would have been recorded if the original time point coincided with the reference. The estimation of new voxel intensity values at the non-measured time point (reference point) is possible by using measured voxels from time points in close proximity. These values are then averaged and weighed by their relative distance, in an interpolative process. The more neighbouring voxels taken into account, the slower it is to compute the interpolative method; however, the more reliable are the estimated values. Hence, the interpolative method must be chosen carefully. In our study, we opted to use a *sinc* interpolation seeing that it offered a better compromise between spent time and results reliability.

Appendix 4: Head Motion Detection and Correction

In Head motion detection and correction, the six parameters (three for translation and three for rotation) which characterize the alignment movements that a single slice should undergo in order to better fit the reference volume, are estimated iteratively using a standard optimization algorithm. With this method, the differences in corresponding condition's intensity values between the reference volume and the transforming one are continuously calculated. The iterative adjustment of these values stops if no further improvement can be achieved, i.e. when a minimum has been found and assigned to one of the parameters. These final parameters are then applied to the transforming volume, thus creating a new one that will replace it in the motion corrected data set. *BrainVoyager QX* displays the six motion parameters in a line plot (similar to the one in Figure 7.2), enabling us to guarantee plausible results by checking if motion correction worked effectively.

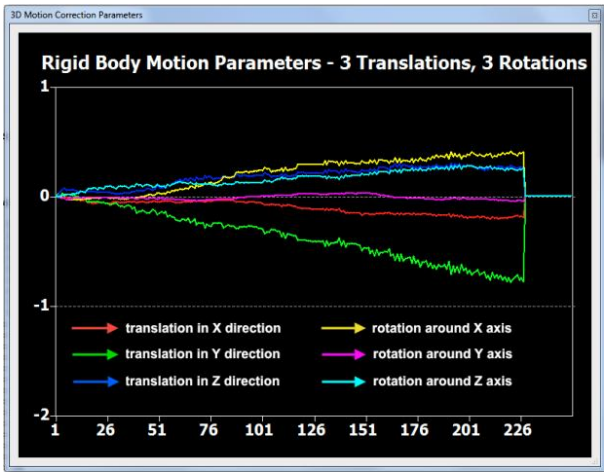

Figure 7.2: Rigid Body Motion Parameters plot shown automatically by BrainVoyager after Head motion detection and correction (image collected from BrainVoyager's User Guide)

Appendix 5: Removal of Linear and Non-linear trends

While removing linear and non-linear trends, *BrainVoyagerQX* offers the possibility of using several filters, from which the high-pass filter using general linear model approach with Fourier basis set is recommended.

The general linear model (GLM) is a statistical technique used, in this case, to estimate the contributions of low frequencies to each voxel's time courses (a more detailed definition of this statistical method can be found in sub-chapters 1.6 and 2.3). Provided a design matrix with the appropriate set of predictors, the GLM estimates a beta values for each predictor. The sum of all predictors, weighted by the corresponding estimated beta value, should produce a time course as close as possible to the measured in original data.

The chosen design matrix dictates the filter's cut-off value, i.e. the lowest frequency value kept in the voxel's time course (all frequency values below the cut-off value will be removed). This design matrix's cut-off value is usually specified by sine and cosine waves, whose cycles fall within the extent of the fMRI data.

The resulting time course, predicted by GLM, is subtracted from the original data, resulting in a filtered time course containing only frequencies above the specified cut-off value. Figure 7.3 shows an example time course in which the blue curve represents the original data, the green lines is the fit of the GLM and the magenta curve corresponds to the filtered resulting data.

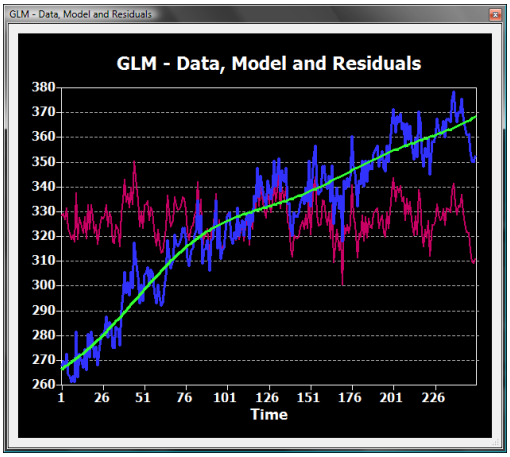

Figure 7.3: Example time course that shows the variation in signal's drift before and after Removal of Linear and non-linear trends. The blue curve represents the original data, the green line is the fit of the GLM and the magenta curve corresponds to the filtered resulting data (image collected from BrainVoyager's User Guide)

.

Appendix 6: Talairach Transformation of Anatomical Data

Talairach coordinates are defined directly in the structural data, through manual identification of the anterior (AC) and posterior (PC) commissures. After the AC-PC plane is identified, the anatomical image undergoes translations and rotations, becoming aligned with it. From that point, the x-axis initiates in the left hemisphere and extends itself to the right hemisphere through AC, whereas the *z*-axis runs from the inferior part of the brain, through the AC, until brain's superior section.

Since every brain has its own dimensions, the next crucial step is the specification of cerebrum borders. By manually identifying brain's uppermost and lower points, as well as its left, right, anterior and posterior extremities, a cuboid is generated which encloses the cortex, running parallel to the three previously defined axis. This bounding box is automatically sub-divided by sub-planes in twelve sub-cuboids as represented in Figure 7.4.

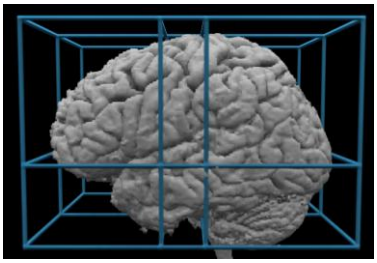

Figure 7.4: Talairach Transformation's 3D cuboid representation (image collected from BrainVoyager's User Guide)

Each one of the sub-cuboids suffers linear alterations, such as expansion and shrinkage, to match the size of the corresponding sub-cuboid of the standard *Talairach* brain (from Talairach & Tournoux (1988)). This final step allows a successful fitting of the anatomical data in the Talairach space.

Once the brain is in the *Talairach* space, it is crucial to verify if the transformed subject brain matches perfectly to the *Talairach* standard boundaries, which can be achieved by choosing to display a grind system of the *Talairach* space superimposed to the transformed anatomical data.

Appendix 7: Intensity Inhomogeneity Correction

IIHC follows four important steps that, even though simple, may prove to be tremendously time-consuming when manually handled.

The first step is Background Cleaning which consists in setting to zero the intensity of all the voxels in the background image. Since not all background voxels have the same intensity values, especially due to "salt and pepper" noise, their identification is hampered, thus leading to an incomplete background cleaning. For that reason, an additional binarization of the 3D anatomical image must be implemented, in which all voxels with intensity values higher than zero are ser to the same integral value (typically 240 which is visualized as "blue"). In result, a 3D image with black background and various scattered blue clusters is formed. Knowing that the largest blue cluster corresponds to the head/brain, its identification and the subsequent setting of all other connected components to zero, will allow the accomplishment of a 3D anatomical image with perfectly cleaned background.

In the second step, the cleaned and still binarized 3D anatomical image is eroded in its perimeter. This erosion breaks intensity connections between the brain and the surrounding head tissue, allowing the differentiation of the head/brain cluster into two separate connected components. Since the larger of the two mentioned clusters usually corresponds to the brain, setting the remaining cluster's voxels to zero will result in a 3D binarized image whose sole cluster contains only brain voxels. However, as the erosion process is anything but rigorous, the extracted cluster will correspond to a "shrunken" version of the actual imaged brain. Therefore, a dilatation operation (that actually consists in inverting the erosion process) must be run in order to re-add the previously cropped brain's fringe. At that point, the image of the extracted brain solely presents voxels assigned to white and grey matters.

The following step of IIHC encompasses the detection of white matter. Nonetheless, this is not an easy task, seeing that there may be grey matter's voxels with high intensity values and white matter's voxels with low intensity values, owing to the existence of regions in which the SNR values were higher

and lower, respectively (due to spatial inhomogeneities). In order to counteract this barrier, *BrainVoyager*'s automatic IIHC tool will begin by analyzing blocks of 125 voxels (N = 5 x 5 x 5 = 125) and heuristically investigate their intensity values distribution. The examination of each block is performed using the trimmed range statistic, an estimation process that allows the exclusion of some of the extreme values of a certain statistical distribution. More precisely, the intensity values for each local distribution of N voxels are ranked in increasing order, x_i, and the median intensity, $X_{N/2}$, is calculated. Thenceforth, for each voxel within one block, there will be a distinctive normalized value, y_i, obtained with resource to Equation 7.5.

$$y_i = \frac{x_i}{2\,X_{N/2}}$$

Equation 7.5

The trimmed range statistic, r, for each local distribution can be calculated using Equation 7.6 for $1 < j < k < N$ (with $j = 2$ and $k = N - 1$ in current implementation).

$$r = y_k - y_j$$

Equation 7.6

Basically, the trimmed range value characterizes the variability of voxel's intensity within one block. If this value is smaller than a specific tissue range threshold (by default 0.25), the block shows low intensity variability and therefore it is plausible to assume that it stems from only one tissue type. The residual local blocks, whose r values exceed the mentioned threshold, are considered to encompass multiple tissues types, thus, they are not further taken into account in white matter detection. The surviving blocks are those with more homogeneous intensity distribution across their voxels. Their median values are

then ranked in increasing order with further discarding of a specific percentile (30% by default) of the blocks with lower median intensities. Finally, the voxels of the remaining blocks are labelled as white matter. Although heuristic, this method shows valid results, especially when repeated several times.

The final step in automatic IIHC is bias field estimation within the labelled white matter voxels. In this approach, low-order polynomials (default order: 3) are used to capture white matter's intensities variation across the 3D image space. With resource to singular value decomposition combined with least squares method (statistical approaches that intend to minimize the sum of squared residuals, i.e. the difference between an observed value and the fitted value provided by a model) the polynomials are bind to the extracted white matter cluster, thus allowing the creation of a bias field with the estimated parameters of low-frequency fluctuations across the 3D image's space that may be seen in Figure 7.5's lower right side. Finally, the polynomials are removed from the data originating an new 3D anatomical image whose voxels have much more homogeneous intensities (grey matter intensities will be centred around intensity "100" and white matter intensities around "160" by default).

As can be seen in Figure 7.5's upper right side, this IIHC tool improves anatomical data's visualization and creates better starting points for subsequent segmentation tools.

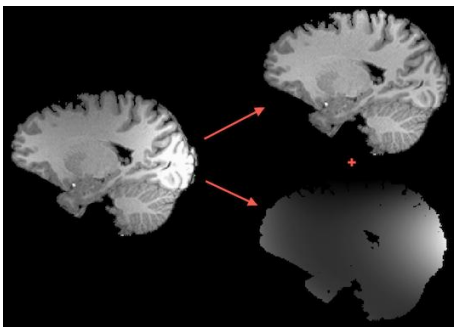

Figure 7.5: Representation of Bias Field Estimation and final result obtain with BrainVoyager's Automatic Intensity Inhomogeneities Correction (collected from BrainVoyager QX user guide)

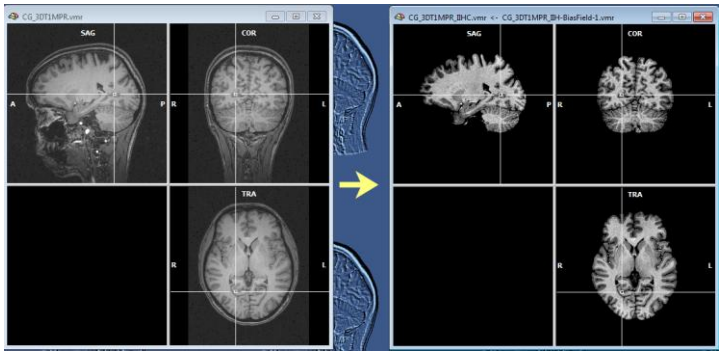

Figure 7.6: Initial 3D anatomical data (left side) counterposed with the 3D anatomical image obtained after Intensity Inhomogeneities Correction with BrainVoyager's automatic tool (collected from BrainVoyager QX user guide)

8

References

ADDIS, Donna Rose, WONG, Alana T., SCHACTER, Daniel L. - *Remembering the past and Imagining the Future: Common and Distinct Neural Substrates during Event Construction and Elaboration*. *Neuropsychologia* 45.7 (2007): 1363-377.

AMINOFF, Michael J., DAROFF Robert B. - *Encyclopedia of the Neurological Sciences*. Massachusetts, USA: Academic Press, 2nd edition.2014.ISBN 978-0123851574

ANDREESCU, Carmen, GROSS, James J., LENZE, Eric *et al. - Altered Cerebral Blood Flow Patterns Associated with Pathologic Worry in the Elderly*. Depression and Anxiety 28.3 (2011): 202-09.

ANDREWS-HANNA, Jessica R., SAXE, Rebecca, YARKONI, Tal - *Contributions of Episodic Retrieval and Mentalizing to Autobiographical Thought: Evidence from Functional Neuroimaging, Resting-state Connectivity, and FMRI Meta-analyses.* NeuroImage. 91 (2014): 324-35.

BALDO, Juliana V., WILKINS, David P., OGAR, Jennifer *et al. - Role of the Precentral Gyrus of the Insula in Complex Articulation*. Cortex 47.7 (2011): 800-07.

BERENBAUM, Howard - *An Initiation–termination Two-phase Model of Worrying*. Clinical Psychology Review 30.8 (2010): 962-75.

BERMPOHL, Felix, PASCUAL-LEONE, Alvaro, AMEDI, Amir *et al. – Attentional Modulation of Emotional Stiulus Processing: An FMRI Study using Emotional Expectancy*. Human Brain Mapping 27.8 (2006): 662-77.

BOTZUNG, Anne, DENKOVA, Ekaterina, MANNING, Lilianne - *Experiencing past and Future Personal Events: Functional Neuroimaging Evidence on the Neural Bases of Mental Time Travel*. Brain and Cognition 66.2 (2008): 202-12.

CARTER, Ronald Mckell, O'DOHERTY, John P., SEYMOUR, Ben - *Contingency Awareness in Human Aversive Conditioning Involves the Middle Frontal Gyrus*. NeuroImage 29.3 (2006): 1007-012.

CIARAMITARO, V. M., BURACAS, G. T., BOYNTON, G. M. – *Spatial and Cross-Modal Attention Alter Responses to Unattended Sensory Information in Early Visual and Auditory Human Cortex.* Journal of Neurophysiology 98.4 (2007):2399-413.

DAVEY, Graham, WELLS, Adrian. *Worry and Its Psychological Disorders: Theory, Assessment, and Treatment*. Chichester, England: Wiley, 1st edition. 2006. ISBN 978-04700127796

DESCHAMPS, Isabelle, BAUM, Shari R., GRACCO, Vincent L. - *On the Role of the Supramarginal Gyrus in Phonological Processing and Verbal Working Memory: Evidence from RTMS Studies*. Neuropsychologia 53 (2014): 39-46.

ENGELS, Anaa S., HELLER, Wendy, MOHANTY *et al. – Specificity of Regional Brain Activity in Anxiety Types during Emotion Processing.* Psychophysiology 44.3 (2007): 352-63

FORMISANO, E., SALLE, Francesco D., GOEBEL, Rainer - *Fundamentals of data analysis methods in fMRI.* In: LANDINI, Luigi, POSITANO, Vicenzo, SANTARELLI, Maria F. - *Advanced Image processing in magnetic resonance imaging*. Florida, USA: CRC Press, 1st edition. 2005. ISBN 978-0-8247-2542-6. 481-503

FRISTON, K. J., HOLMES, A. P., WORSLEY, K. J. *et al.- Statistical Parametric Maps in Functional Imaging: A General Linear Approach.* Human Brain Mapping 2.4 (1994): 189-210.

GARNER, Matthew, MÖHLER, Hanns, STEIN, Dan J. *et al. – Research in Anxiety Disorders: From the Bench to the Bedside.* European Neurophychopharmacology 19.6 (2009): 381-90.

GRAHN, Jessica A., PARKINSON, John A., OWEN, Adrian M. - *The Cognitive Functions of the Caudate Nucleus*. Progress in Neurobiology 86.3 (2008): 141-55.

GREENE,, Sarah J., KILLIANY, Ronald J. - *Subregions of the Inferior Parietal Lobule Are Affected in the Progression to Alzheimer's Disease*. Neurobiology of Aging 31.8 (2010): 1304-311.

GRINDROD, Christopher M., BILENKO, Natalia Y., MYERS, Emily B. *et al. - The Role of the Left Inferior Frontal Gyrus in Implicit Semantic Competition and Selection: An Event-related FMRI Study*. Brain Research 1229 (2008): 167-78.

HOEHN-SARIC, Rudolf, LEE, Jae Sung, MCLEOD, Daniel R. *et al. - Effect of Worry on Regional Cerebral Blood Flow in Nonanxious Subjects*. Psychiatry Research: Neuroimaging 140.3 (2005): 259-69.

HOFMANN, Stefan G., MOSCOVITCH, David A., LITZ, Brett T. *et al. - The Worried Mind: Autonomic and Prefrontal Activation During Worrying*. Emotion 5.4 (2005): 464-75.

HUETTEL, Scott A., SONG, Allen W., MCCARTHY, Gregory - *Functional Magnetic Resonance Imaging*. Massachusetts, USA: Sinauer Associates, 2nd edition. 2009. ISBN 978-0-87893-286-3

JIN, Guangwei, LI, Kuncheng, QIN, Yulin *et al. - FMRI Study in Posterior Cingulate and Adjacent Precuneus Cortex in Healthy Elderly Adults Using Problem Solving Task*. Journal of the Neurological Sciences 318.1-2 (2012): 135-39.

JONES, Rhiannon, BHATTACHARYA, Joydeep. - *A Role for the Precuneus in Thought–action Fusion: Evidence from Participants with Significant Obsessive–compulsive Symptoms*. NeuroImage: Clinical 4 (2014): 112-21.

JUNG-BEEMAN, Mark - *Bilateral Brain Processes for Comprehending Natural Language*. Trends in Cognitive Sciences 9.11 (2005): 512-18.

KALISCH, Raffael, GERLICHER, Anna M.V. - *Making a Mountain out of a Molehill: On the Role of the Rostral Dorsal Anterior Cingulate and Dorsomedial Prefrontal Cortex in Conscious Threat Appraisal, Catastrophizing, and Worrying*. Neuroscience & Biobehavioral Reviews 42 (2014): 1-8.

HONHKEUN, Kim - *A Dual-subsystem Model of the Brain's Default Network: Self-referential Processing, Memory Retrieval Processes, and Autobiographical Memory Retrieval*. NeuroImage 61.4 (2012): 966-77.

KOENIGS, M., A., BARBEY, K., POSTLE, B. R. *et al. - Superior Parietal Cortex Is Critical for the Manipulation of Information in Working Memory*. Journal of Neuroscience 29.47 (2009): 14980-4986.

KORNAK, John. *Spatially Extended FMRI Signal Response to Stimulus in Non-Functional Relevant Regions of the Human Brain: Preliminary Results.* The Open Neuroimaging Journal 5.1 (2011): 24-32.

KRIEGESKORTE, N., GOEBEL, R., BANDETTINI, P. - *Information-based functional brain mapping*. PNAS 103 (2006): 3863-3868.

KÜBLER, Andrea, DIXON, Veronica, GARAVAN, Hugh – *Automaticity and Reestablishment of Executive Control – An FMRI Study.* Journal of Cognitive Neuroscience 18.8 (2006): 1331-342.

LANCASTER, J. L., RAINEY, L.H., SUMMERLIN, J.L., *et al. - Automated labeling of the human brain: A preliminary report on the development and evaluation of a forward-transform method*. Human Brain Mapp 5 (1997): 238-242.

LANCASTER, J.L., WOLDORFF, M.G., PARSONS L.M. *et al. - Automated Talairach Atlas labels for functional brain mapping*. Human Brain Mapping 10 (2000): 120-131.

LI, Wei, QIN, Wen, LIU, Huaigui *et al. - Subregions of the Human Superior Frontal Gyrus and Their Connections*. NeuroImage 78 (2013): 46-58.

LIAKAKIS, G., NICKEL, J., SEITZ R.J. - *Diversity of the Inferior Frontal Gyrus—A Meta-analysis of Neuroimaging Studies*. Behavioural Brain Research225.1 (2011): 341-47.

LINDQUIST, Martin A. – *The Statstical Analysis of FMRI Data.* Statistical Science 23.4 (2008): 439-64.

LOGOTHETIS, Nikos K. - *What We Can and What We Can't Do with FMRI*. Society for Neuroscience. Society for Neuroscience, 2012.

LUNDSTROM, Brian Nils, INGVAR, Martin, PETERSON, Karl Magnus - *The Role of Precuneus and Left Inferior Frontal Cortex during Source Memory Episodic Retrieval*. NeuroImage 27.4 (2005): 824-34.

MADDOCK, Richard J., GARRETT, Amy S., BUONOCORE, Michael H. - *Posterior Cingulate Cortex Activation by Emotional Words: FMRI Evidence from a Valence Decision Task*. Human Brain Mapping 18.1 (2003): 30-41.

MADDOCK, Richard J., BUONOCORE, Michael H. - *Activation of Left Posterior Cingulate Gyrus by the Auditory Presentation of threat-related Words: An FMRI Study*. Psychiatry Research: Neuroimaging 75.1 (1997): 1-14.

MALOUIN, Francine, RICHARDS, Carol L., JACKSON. Philip L. *et al. - Brain Activations during Motor Imagery of Locomotor-related Tasks: A PET Study*. Human Brain Mapping 19.1 (2003): 47-62.

MCKEON, M.J., MAKEIG, S., BROWN, G.G. *et al. - Analysis of fMRI data by blind separation into independent spatial components*. Humain Brain Map 6 (1998):160-188.

MORENO-PERAL, P., CONEJO-CERON, S., MOTRICIO, E. *Et al.* al. - *Risk factors for the onset of panic and generalized anxiety disorders in the general adult population. A systematic review of cohort studies*. J Affect Disord 168 (2014): 337–348.

NISHITANI, Nobuyuki, NAGAMINE, Takashi, SHIBASAKI, Hiroshi. - *Modality-specific Subregions in Human Inferior Parietal Lobule: A Magnetoencephalographic Study during Cognitive Tasks*. Neuroscience Letters 252.2 (1998): 79-82.

OKUDA, Jiro, FUJII, Toshikatsu, OHTAKE, Hiroya *et al. - Thinking of the Future and Past: The Roles of the Frontal Pole and the Medial Temporal Lobes*. NeuroImage 19.4 (2003): 1369-380.

PAULESU, E., SAMBUGARU, E., TORTI, T. *Et al. - Neural Correlates of Worry in Generalized Anxiety Disorder and in Normal Controls: A Functional MRI Study*. Psychological Medicine 40.01 (2010): 117

POSNER, M. I., GILBERT, C. D. – *Attention and Primary Visual Cortex.* Proceedings of the National Academy of Sciences 96.6 (1999): 2585-587.

GOEBEL, R., ESPOSITO F., FORMISANO, E. - *Analysis of FIAC data with BrainVoyager QX: From single-subject to cortically aligned group GLM analysis and self-organizing group ICA*. Human Brain Mapping, 27(5):392–401, 2006.

RESS, David, BACKUS, Benjamin, HEEGER, David – *FMRI Cortical Activity Predicts Pattern-detection Performance.* NeuroImage 11.5 (2000): S3.

ROSE, S., ROWLAND, T., PANNEK, K. *et al. - Structural Hemispheric Asymmetries in the Human Precentral Gyrus Hand Representation*. Neuroscience 210 (2012): 211-21.

SEGER, C. A. - *The Roles of the Caudate Nucleus in Human Classification Learning*. Journal of Neuroscience 25.11 (2005): 2941-951..

SILVER, M. A, RESS D., HEEGER D. J. – *Neural Correlates of Sustained Spatial Attention in Human Early Visual Cortex.* Journal of Neurophysiology 97.1 (2007): 229-37.

SQUIRE, Larry R., STARK, Gaig E. L., CLARCK, Robert E. – *The Medial Temporal Lobe.* Annual Review of Neuroscience 27.1 (2004): 279-306.

SZPUNAR, K. K., WATSON, J. M., MCDERMOTT, K. B. - *Neural Substrates of Envisioning the Future*. Proceedings of the National Academy of Sciences104.2 (2007): 642-47.

TALAIRACH, J., TOURNOUX, Pierre - *Co-planar Stereotaxic Atlas of the Human Brain: 3-dimensional Proportional System: An Approach to Cerebral Imaging*. Stuttgart, Germany: G. Thieme, 1st edition. 1988. ISBN 978-0865772939

TSUJII, Takeo, SAKATANI, Kaoru, MASUDA, Sayako *et al. - Evaluating the Roles of the Inferior Frontal Gyrus and Superior Parietal Lobule in Deductive Reasoning: An RTMS Study*. NeuroImage58.2 (2011): 640-46.

VIARD, Armelle, CHÉTELAT, Gäel, LEBRETON, Karine *et al.* – *Mental Time Travel into the Past and the Future in Healthy Aged Adults: An FMRI Study.* Brain and Cognition 75.1 (2011): 1-9.

WESTERLUND, Masha, PYLKKÄNEN, Liina. - *The Role of the Left Anterior Temporal Lobe in Semantic Composition vs. Semantic Memory*. Neuropsychologia57 (2014): 59-70.

ZHAN, Sheng, CHIANG-SHAN R. L. - *Functional Connectivity Mapping of the Human Precuneus by Resting State FMRI*. NeuroImage 59.4 (2012): 3548-562.